Hindawi
Journal of Mathematics
Volume 2022, Article ID 9999070, 20 pages
https://doi.org/10.1155/2022/9999070

Research Article

A Highly Accurate Technique to Obtain Exact Solutions to Time-Fractional Quantum Mechanics Problems with Zero and Nonzero Trapping Potential

Muhammad Imran Liaqat,[1] **Adnan Khan**,[1] **Md. Ashraful Alam**,[2] **and M. K. Pandit**[2]

[1]*National College of Business Administration and Economics, Lahore, Pakistan*
[2]*Department of Mathematics, Jahangirnagar University, Savar, Dhaka, Bangladesh*

Correspondence should be addressed to Md. Ashraful Alam; ashraf_math20@juniv.edu

Received 5 March 2022; Revised 20 March 2022; Accepted 20 April 2022; Published 31 May 2022

Academic Editor: Mawardi Bahri

In this study, the highly accurate analytical Aboodh transform decomposition method (ATDM) in the sense of Caputo fractional derivative is used to determine the approximate and exact solutions of both linear and nonlinear time-fractional Schrodinger differential equations (SDEs) with zero and nonzero trapping potential that describe the nonrelativistic quantum mechanical activity. The Adomian decomposition method (ADM) and the Aboodh transform of Caputo's fractional derivative are combined in this method. The recurrence and absolute error of the four problems are analyzed to evaluate the efficiency and consistency of the presented method. In addition, numerical results are also compared with other methods such as the fractional reduced differential transform method (FRDTM), the homotopy analysis method (HAM), and the homotopy perturbation method (HPM). The results obtained by the proposed method show excellent agreement with these methods, which indicates its effectiveness and reliability. This technique has the benefit of not requiring any minor or major physical parameter assumptions in the problem. As a result, it may be used to solve both weakly and strongly nonlinear problems, overcoming some of the inherent constraints of classic perturbation approaches. To solve nonlinear fractional-order differential equations, just a few computations are necessary. As a consequence, it outperforms homotopy analysis and homotopy perturbation approaches significantly. The procedure is quick, precise, and easy to implement. Convergence analysis of the series solution is also offered.

1. Introduction

The shortcoming of classical mechanics to explain several physical processes, including those on microscopic scales, such as the photoelectric effect, black body radiation, and atomic stability, led to the development of modern quantum mechanics. It is explained by the fact that all physical quantities of a bound system are confined to discrete value quantization. Quantum mechanics may successfully describe various modern physics processes in atomic and nuclear physics, as well as other fields of modern physics, where the Schrödinger equation can be used to describe the behavior of electrons in atomic physics and nucleons in nuclear physics [1]. This equation was developed by Austrian physicist Erwin Schrodinger in late 1925 and published in 1926.

Fractional partial differential equations (PDEs), which are an extension of integer-order PDEs, have subsequently received much interest. They can be used to extract memory and hereditary qualities from a variety of materials and processes. Fractional PDEs such as the Boussinesq equation, Korteweg-de Vries equation, Schrodinger equation, Burger's equation, and others are frequently used to describe varied nonlinear wave processes in mechanics, physics, biology, chemistry, and other areas [2]. The time-fractional SDE is the fundamental physics equation for characterizing nonrelativistic quantum mechanical activity. Electromagnetic waves, quantitative finance, quantum development of

complex systems, and dielectric polarization have all been pulled into the time-fractional SDE in recent years [3, 4].

We examined the exact and numerical approaches to comprehend the physical mechanism of such a natural phenomenon. As a result, we are looking for a mathematical solution to PDEs that is both precise and numerical. Many papers have focused on constructing solutions to PDEs through well-known methods. Lie symmetry analysis [5], inverse scattering approach [6], spectral collocation method [7], Hirota method [8], Backlund transformation method [9], Modified Kudryashov method [10], Laplace transform coupled with Adomian decomposition method [11], Elzaki residual power series method [12], adaptation on power series method with conformable operator [13], Legendre wavelet method [14] and modified conformable Shehu transform decomposition method [15] are some of the most effective and efficient methods.

Differential equations (DEs), partial integrodifferential equations (PIDs), and delayed differential equations (DDEs) are all solved by employing integral transforms, which are among the most valuable techniques in mathematics. The conversion of DEs and integral equations into terms of a simple algebraic equation is enabled by the appropriate selection of integral transforms. The origins of integral transforms can be traced back to P. S. Laplace's work in the 1780s and Joseph Fourier's work in 1822. In the beginning, ordinary and PDEs were solved using the Laplace transform and the Fourier transform which are two well-known transforms. These modifications were then applied to fractional-order DEs in the domain of fractional calculus [16–19]. In recent years, researchers have proposed lots of new different transformations to solve a variety of mathematical problems. Fractional-order DEs are solved using the Laplace transform [20], fractional complex transform [21], travelling wave transform [22], Elzaki transform [23], Sumudu transforms [24], and ZZ transforms [25], among others. These transformations are paired with additional analytical, numerical, or homotopy-based techniques to handle fractional-order DEs.

The general state of quantum mechanics equations, which are commonly described as fractional-order SDEs, will be solved in this study using an appealing and effective analytical technique, the Aboodh transform decomposition method (ATDM). The Aboodh transform was established in 2013 by Khalid Aboodh to facilitate solving ordinary DEs and PDEs in the time domain [26]. The Aboodh transform is generated using the traditional Fourier integral. The Elzaki transform and the Laplace transform are intimately related to this integral transform. The A-T, which has been used by several researchers for fractional-order DEs [27–31], has recently caught the interest of many mathematicians.

We analyze then on linear time fractional-order SDE with zero trapping potential in its more general version, which is represented by the complex-valued function $\xi(\varpi, \tau)$ of the form [32].

$$iD_\tau^\nu \xi(\varpi, \tau) + D_{\varpi\varpi}\xi(\varpi, \tau) + \eta|\xi(\varpi, \tau)|^{2\lambda}\xi(\varpi, \tau) = 0, \tag{1}$$

where $\eta \in R$, $0 < \nu \leq 1$, $i = \sqrt{-1}$, D_τ^ν indicates Caputo fractional derivative of order ν, $\xi(\varpi, \tau)$ is the unknown complex-valued function to be determined, $\varpi \in R$, $\tau \geq 0$, and $|\xi(\varpi, \tau)|$ represent the modulus of $\xi(\varpi, \tau)$; with the following initial and boundary conditions given by $\xi(\varpi, 0) = \Upsilon(\varpi)$, $\xi(0, \tau) = A(\varpi)$, and $\xi_\varpi(0, \tau) = B(\varpi)$.

The time-fractional nonlinear SDE with nonzero trapping potential has the following form [33]:

$$iD_\tau^\nu \xi(\varpi, \tau) = -\frac{1}{2}\mathfrak{J}_\varpi \xi(\varpi, \tau) + \Theta(\varpi)\xi(\varpi, \tau) + H_d Q(\xi(\varpi, \tau)), \quad \tau \geq 0,\ 0 < \nu \leq 1,\ \varpi \in R, \tag{2}$$

with the initial condition:

$$\xi(\varpi, 0) = \Upsilon(\varpi), \tag{3}$$

where $\varpi \in R$, $\Theta_d(\varpi)$ is the trapping potential and H_d is a real constant $\mathfrak{J}_\varpi$ is a linear operator, $Q(\xi(\varpi, \tau))$ is a nonlinear function, and D_τ^ν is the Caputo fractional differential operator.

The physical model (2) and its generalized forms arise in various areas of physics, including nonlinear optics, plasma physics, superconductivity, and quantum mechanics [34].

The time-fractional SDE has been investigated through various methods, such as the homotopy perturbation method [35], exponential rational function method [36], residual power series method [37], modified transformation method [38], two-dimensional differential transform method [39], extended simple equation method [40], trigonometric B-spline method [41], fractional reduced differential transform method [42], and homotopy analysis method [43]. All these methods have their own specific limits and deficiencies. These methods require enormous computational work and high running times. In this study, we used the simple and efficient technique known as the ATDM to solve the SDE of the fractional derivative in the sense of Caputo. The recommended method is simple to use and can be applied to both linear and nonlinear problems. It also has the ability to reduce the complexity of the computational effort. The set of rules of ATDM depends on converting the SDE into Aboodh transform space and, after converting the SDE into an algebraic equation, applying inverse A-T and then introducing a series of solutions to the obtained algebraic equation, at the final step, obtaining the target result through the iteration process.

The structure of the paper is as follows: we will employ various fundamental definitions and results from fractional calculus theory in the next section. The primary idea of the ATDM is investigated in Section 3 in order to establish fractional SDE solutions. Section 4 demonstrates the method's potential, capability, and simplicity by obtaining approximate and exact solutions to four SDE problems. The proposed method is illustrated numerically and graphically in Section 5, and the numerical results are evaluated in Section 5. The conclusion is covered in Section 6.

Table 1: The absolute error in ATDM and FRDTM for Example 1 at $\nu = 1$.

τ	Real part [ATDM] Abs. error	Img. part [ATDM] Abs. error	Real part [FRDTM] Abs. error	Img. part [FRTDM] Abs. error
0.2	0	$2.775557561562891 \times 10^{-17}$	0	$2.775557561562891 \times 10^{-17}$
0.4	$3.508304757815494 \times 10^{-14}$	$6.661338147750939 \times 10^{-16}$	$3.508304757815494 \times 10^{-14}$	$6.66133814775093 \times 10^{-16}$
0.6	$4.540257059204578 \times 10^{-12}$	$1.743050148661495 \times 10^{-14}$	$4.540257059204578 \times 10^{-12}$	$1.743050148661495 \times 10^{-14}$
0.8	$1.43222100845719 \times 10^{-10}$	$1.645683589401869 \times 10^{-12}$	$1.43222100845719 \times 10^{-10}$	$1.645683589401869 \times 10^{-12}$
1.0	$2.081645966711676 \times 10^{-9}$	$5.585931717178028 \times 10^{-11}$	$2.081645966711676 \times 10^{-9}$	$5.585931717178028 \times 10^{-11}$

2. Basic Concepts and Representations in Fractional Calculus Theory

Fractional calculus is a modified version of classical calculus. Fractional calculus can explain a wide range of complex phenomena, including memory and heredity. This subject has drawn many researchers because of its worldwide aspect and numerous applications in several domains of science, such as physics, signal processing, modeling, control theory, economics, and chemistry [44, 45]. In this section, we covered some definitions and basic features of fractional calculus theory, as well as the fundamentals of the Aboodh transformation, which will be used later in this paper.

Definition 1 (see [43]). The Aboodh transform (A-T) for function $\xi(\tau)$ of exponential order over the set of functions is defined as

$$R = \left\{\xi(\tau) | \exists M,\ u_1,\ u_2 > 0,\ |\xi(\tau)| < Me^{-\hbar\tau}\right\}, \tag{4}$$

where M is a finite number and u_1, u_2 may be finite or infinite. A-T is denoted by the operator $A[.]$ and defined as

$$A[\xi(\tau)] = Q(\hbar) = \frac{1}{\hbar}\int_0^{\infty} \xi(\tau)e^{-\tau\hbar}\mathrm{d}\tau,\ \tau \geq 0,\ u_1 \leq \hbar \leq u_2. \tag{5}$$

Definition 2 (see [46]). The Inverse A-T of function $\xi(\tau)$ is denoted by $A^{-1}[Q(\hbar)]$ and defined as

$$A^{-1}[Q(\hbar)] = \xi(\tau) = \frac{1}{2\pi i}\int_{w-i\infty}^{w+i\infty} \hbar e^{\hbar\tau}Q(\hbar)\mathrm{d}\hbar. \tag{6}$$

A-T of several functions can be seen in Table 1 [27–29]. A-T for some elementary functions is given as

$$\begin{aligned} &\xi(\tau)Q(\hbar) = A[\xi(\tau)] \\ &1\frac{1}{\hbar} \\ &\tau\frac{1}{\hbar^2} \\ &\tau^{\alpha}\frac{\alpha!}{\hbar^{\alpha+2}},\ \alpha = 1, 2, \ldots \\ &\tau^{\nu}\frac{\Gamma(\nu+1)}{\hbar^{\nu+2}}. \end{aligned} \tag{7}$$

Definition 3 (see [47]). The Caputo fractional derivative of order $\nu > 0$ is defined by

$$D_{\tau}^{\nu}\xi(\tau) = \begin{cases} \dfrac{\mathrm{d}^{\alpha}}{\mathrm{d}\tau^{\alpha}}\xi(\tau),\ \alpha = \nu \in N, \\ \dfrac{1}{\Gamma(\alpha-\nu)}\displaystyle\int_0^{\tau}(\tau-\rho)^{\alpha-\nu-1}\xi^{(\alpha)}(\rho)d\rho,\ \alpha-1 < \nu < \alpha. \end{cases} \tag{8}$$

We have a few properties of Caputo's fractional derivative.

$$\begin{aligned} &D_{\tau}^{\nu_1}D_{\tau}^{\nu_2}\xi(\tau) = D_{\tau}^{\nu_1+\nu_2}\xi(\tau), \\ &D_{\tau}^{\nu}C = 0,\ C \in R, \\ &D_{\tau}^{\nu}(\tau-\eta)^{\beta} = \frac{\Gamma(\beta+1)}{\Gamma(\beta+1-\nu)}(\tau-\eta)^{\beta-\nu}, \\ &\qquad \alpha-1 < \nu \leq \alpha,\ \beta > \alpha-1,\ \alpha \in N,\ \beta \in R, \\ &D_{\tau}^{\nu}\left(C_1\xi_1(\tau) + C_2\xi_2(\tau)\right) = C_1D_{\tau}^{\nu}\xi_1(\tau) + C_2D_{\tau}^{\nu}\xi_2(\tau),\ C_1, C_2 \in R. \end{aligned} \tag{9}$$

i. $D_{\tau}^{\nu}(J_{\tau}^{\nu}\xi(\tau)) = \xi(\tau)$, J_{τ}^{ν} is the R-L integral of $\xi(\tau)$ order ν.

Lemma 1 (see [27–31]). *If $\xi_1(\tau)$ and $\xi_2(\tau)$ are piecewise continuous on $[0, \infty)$ and are of exponential order $A[\xi_1(\tau)] = Q_1(\hbar)$, $A[\xi_2(\tau)] = Q_2(\hbar)$, and C_1, C_2 are constants, then the properties mentioned below are valid:*

$$\begin{aligned} &A\left[C_1\xi_1(\tau) + C_2\xi_2(\tau)\right] = C_1Q_1(\hbar) + C_2Q_2(\hbar), \\ &A^{-1}\left[C_1Q_1(\hbar) + C_2Q_2(\hbar)\right] = C_1\xi_1(\tau) + C_2\xi_2(\tau), \\ &A\left[D_{\tau}^{\nu}\xi(\tau)\right] = \hbar^{\nu}Q(\hbar) - \sum_{\kappa=0}^{\alpha-1}\frac{\xi^{(\kappa)}(0)}{\hbar^{\kappa-\nu+2}}, \\ &\qquad \alpha-1 < \nu \leq \alpha,\ \alpha \in N. \end{aligned} \tag{10}$$

3. Analysis of the Aboodh Transform Decomposition Method

In this section, we derive the main algorithms of the ATDM separately for the time-fractional Schrodinger differential equation with zero and nonzero trapping potential. The convergence analysis of the expansion solution is also presented.

To present the ATDM on the general SDE with zero trapping potential given in equation (1), we first rewrite equation (1) as

$$D_\tau^\nu \xi(\varpi,\tau) = iD_{\varpi\varpi}\xi(\varpi,\tau) + i\eta|\xi(\varpi,\tau)|^{2\lambda}\xi(\varpi,\tau). \tag{11}$$

Now, applying the A-T to equation (11), we have

$$A\left[D_\tau^\nu \xi(\varpi,\tau)\right] = A\left[iD_{\varpi\varpi}\xi(\varpi,\tau) + i\eta|\xi(\varpi,\tau)|^{2\lambda}\xi(\varpi,\tau)\right]. \tag{12}$$

Using the differentiation property of the A-T and the initial condition of equation (12), we get

$$\begin{aligned}\hbar^\nu A[\xi(\varpi,\tau)] - \frac{\xi(\varpi,0)}{\hbar^{2-\nu}} &= A\left[iD_{\varpi\varpi}\xi(\varpi,\tau)\right] \\ &\quad + A\left[i\eta|\xi(\varpi,\tau)|^{2\lambda}\xi(\varpi,\tau)\right].\end{aligned} \tag{13}$$

$$\begin{aligned}A[\xi(\varpi,\tau)] &= \frac{\xi(\varpi,0)}{\hbar^{2-\nu}} + \frac{1}{\hbar^\nu}A\left[iD_{\varpi\varpi}\xi(\varpi,\tau)\right] \\ &\quad + \frac{1}{\hbar^\nu}A\left[i\eta|\xi(\varpi,\tau)|^{2\lambda}\xi(\varpi,\tau)\right].\end{aligned} \tag{14}$$

Taking the inverse A-T on equation (14), we get as

$$\begin{aligned}\xi(\varpi,\tau) &= A^{-1}\left\{\frac{\xi(\varpi,0)}{\hbar^2}\right\} + A^{-1}\left\{\frac{1}{\hbar^\nu}A\left[iD_{\varpi\varpi}\xi(\varpi,\tau)\right]\right\} \\ &\quad + A^{-1}\left\{\frac{1}{\hbar^\nu}A\left[i\eta|\xi(\varpi,\tau)|^{2\lambda}\xi(\varpi,\tau)\right]\right\}.\end{aligned} \tag{15}$$

So, according to the ATDM, we can acquire the solution $\xi(\varpi,\tau)$ to equation (15) as follows:

$$\xi(\varpi,\tau) = \sum_{\alpha=0}^{\infty}\xi_\alpha(\varpi,\tau). \tag{16}$$

The nonlinear operator is decomposed as

$$\aleph(\xi(\varpi,\tau)) = \sum_{\alpha=0}^{\infty}W_\alpha(\xi_0,\xi_1,\xi_2,\ldots), \tag{17}$$

where

$$W_\alpha = \frac{1}{\alpha!}\frac{\mathrm{d}^\alpha}{\mathrm{d}\lambda^\alpha}\left[\aleph\left(\sum_{\kappa=0}^{\alpha}\lambda^\kappa\xi_\kappa(\varpi,\tau)\right)\right]_{\lambda=0}. \tag{18}$$

The few terms of the decomposed nonlinear terms which are calculated from equation (18) are given as

$$\begin{aligned}W_0 &= \xi_0^2(\varpi,\tau)\overline{\xi(\varpi,\tau)}, \\ W_1 &= \xi_0^2(\varpi,\tau)\overline{\xi_1(\varpi,\tau)} + 2\xi_0(\varpi,\tau)\xi_1(\varpi,\tau)\overline{\xi_0(\varpi,\tau)}, \\ W_2 &= \xi_1^2(\varpi,\tau)\overline{\xi_0(\varpi,\tau)} + 2\xi_0(\varpi,\tau)\xi_2(\varpi,\tau)\overline{\xi_0(\varpi,\tau)} \\ &\quad + 2\xi_0(\varpi,\tau)\xi_1(\varpi,\tau)\overline{\xi_1(\varpi,\tau)} + \xi_0^2(\varpi,\tau)\overline{\xi_0(\varpi,\tau)}.\end{aligned} \tag{19}$$

Now, by replacing equations (18) and (16) with equation (15), we attain as follows:

$$\begin{aligned}\sum_{\alpha=0}^{\infty}\xi_\alpha(\varpi,\tau) &= A^{-1}\left\{\frac{\xi(\varpi,0)}{\hbar^2}\right\} + A^{-1}\left\{\frac{1}{\hbar^\nu}A\left[iD_{\varpi\varpi}\sum_{\alpha=0}^{\infty}\xi_\alpha(\varpi,\tau)\right]\right\} \\ &\quad + A^{-1}\left\{\frac{1}{\hbar^\nu}A\left[i\eta\sum_{\alpha=0}^{\infty}W_\alpha\right]\right\}.\end{aligned} \tag{20}$$

Equating the like terms on both sides of equation (20) yields the general solution of equation (11), which is recursively expressed as

$$\begin{aligned}\xi_0(\varpi,\tau) &= A^{-1}\left\{\frac{\xi(\varpi,0)}{\hbar^2}\right\}, \\ \xi_1(\varpi,\tau) &= A^{-1}\left\{\frac{1}{\hbar^\nu}A\left[iD_{\varpi\varpi}\sum_{\alpha=0}^{\infty}\xi_0(\varpi,\tau)\right]\right\} \\ &\quad + A^{-1}\left\{\frac{1}{\hbar^\nu}A\left[\eta iW_0\right]\right\}, \\ \xi_2(\varpi,\tau) &= A^{-1}\left\{\frac{1}{\hbar^\nu}A\left[iD_{\varpi\varpi}\sum_{\alpha=0}^{\infty}\xi_1(\varpi,\tau)\right]\right\} \\ &\quad + A^{-1}\left\{\frac{1}{\hbar^\nu}A\left[\eta iW_1\right]\right\}, \\ \xi_3(\varpi,\tau) &= A^{-1}\left\{\frac{1}{\hbar^\nu}A\left[iD_{\varpi\varpi}\sum_{\alpha=0}^{\infty}\xi_2(\varpi,\tau)\right]\right\} \\ &\quad + A^{-1}\left\{\frac{1}{\hbar^\nu}A\left[\eta iW_2\right]\right\}, \\ \xi_4(\varpi,\tau) &= A^{-1}\left\{\frac{1}{\hbar^\nu}A\left[iD_{\varpi\varpi}\sum_{\alpha=0}^{\infty}\xi_3(\varpi,\tau)\right]\right\} \\ &\quad + A^{-1}\left\{\frac{1}{\hbar^\nu}A\left[\eta iW_3\right]\right\}, \\ \xi_{\alpha+1}(\varpi,\tau) &= A^{-1}\left\{\frac{1}{\hbar^\nu}A\left[iD_{\varpi\varpi}\sum_{\alpha=0}^{\infty}\xi_\alpha(\varpi,\tau)\right]\right\} \\ &\quad + A^{-1}\left\{\frac{1}{\hbar^\nu}A\left[i\eta\sum_{\alpha=0}^{\infty}W_\alpha\right]\right\}.\end{aligned} \tag{21}$$

where $\alpha = 0, 1, 2, \ldots$

Now, to present the ATDM on the general SDE with nonzero trapping potential given in equation (2), we first rewrite equation (2) as

$$D_\tau^\nu \xi(\varpi,\tau) = -i\left(-\frac{1}{2}\mathfrak{F}_\varpi\xi(\varpi,\tau) + \Theta_d(\varpi)\xi(\varpi,\tau) + H_dQ(\xi(\varpi,\tau))\right). \tag{22}$$

Now, applying the A-T to equation (22), we have:

$$A\left[D_\tau^\nu \xi(\varpi,\tau)\right] = -iA\left(-\frac{1}{2}\mathfrak{F}_\varpi \xi(\varpi,\tau) + \Theta_d(\varpi)\xi(\varpi,\tau) + H_d Q(\xi(\varpi,\tau))\right). \tag{23}$$

Using the differentiation property of the A-T and the initial condition on equation (23), we get

$$\hbar^\nu A[\xi(\varpi,\tau)] - \frac{\xi(\varpi,0)}{\hbar^{2-\nu}} = -iA\left(-\frac{1}{2}\mathfrak{F}_\varpi \xi(\varpi,\tau) + \Theta_d(\varpi)\xi(\varpi,\tau) + H_d Q(\xi(\varpi,\tau))\right). \tag{24}$$

$$A[\xi(\varpi,\tau)] = \frac{\xi(\varpi,0)}{\hbar^2} - \frac{1}{\hbar^\nu} iA\left(-\frac{1}{2}\mathfrak{F}_\varpi \xi(\varpi,\tau) + \Theta_d(\varpi)\xi(\varpi,\tau) + H_d Q(\xi(\varpi,\tau))\right). \tag{25}$$

Taking the inverse A-T on equation (25), we get as

$$\xi(\varpi,\tau) = A^{-1}\left\{\frac{\xi(\varpi,0)}{\hbar^2}\right\} - A^{-1}\left\{\frac{1}{\hbar^\nu} iA\left(-\frac{1}{2}\mathfrak{F}_\varpi \xi(\varpi,\tau) + \Theta_d(\varpi)\xi(\varpi,\tau) + H_d Q(\xi(\varpi,\tau))\right)\right\}. \tag{26}$$

So, according to the ATDM, we can acquire the solution $\xi(\varpi,\tau)$ to equation (26) as follows:

$$\xi(\varpi,\tau) = \sum_{\alpha=0}^{\infty} \xi_\alpha(\varpi,\tau). \tag{27}$$

$$Q(\xi(\varpi,\tau)) = \sum_{\alpha=0}^{\infty} W_\alpha. \tag{28}$$

$$W_\alpha = \frac{1}{\alpha!}\frac{\mathrm{d}^\alpha}{\mathrm{d}\lambda^\alpha}\left[\aleph\left(\sum_{\kappa=0}^{\alpha}\lambda^\kappa \xi_\kappa(\varpi,\tau)\right)\right]_{\lambda=0}. \tag{29}$$

The few terms of the decomposed nonlinear terms which are calculated from equation (29) are given as

$$\begin{aligned} W_0 &= \xi_0^2(\varpi,\tau)\overline{\xi(\varpi,\tau)}, \\ W_1 &= \xi_0^2(\varpi,\tau)\overline{\xi_1(\varpi,\tau)} + 2\xi_0(\varpi,\tau)\xi_1(\varpi,\tau)\overline{\xi_0(\varpi,\tau)}, \\ W_2 &= \xi_1^2(\varpi,\tau)\overline{\xi_0(\varpi,\tau)} + 2\xi_0(\varpi,\tau)\xi_2(\varpi,\tau)\overline{\xi_0(\varpi,\tau)} \\ &\quad + 2\xi_0(\varpi,\tau)\xi_1(\varpi,\tau)\overline{\xi_1(\varpi,\tau)} + \xi_0^2(\varpi,\tau)\overline{\xi_0(\varpi,\tau)}. \end{aligned} \tag{30}$$

Now, by replacing equations (27) and (29) with equation (26), we attain as follows:

$$\sum_{\alpha=0}^{\infty}\xi_\alpha(\varpi,\tau) = A^{-1}\left\{\frac{\xi(\varpi,0)}{\hbar^2}\right\} - A^{-1}\left\{\frac{1}{\hbar^\nu} iA\left(-\frac{1}{2}\mathfrak{F}_\varpi \sum_{\alpha=0}^{\infty}\xi_\alpha(\varpi,\tau) + \Theta_d(\varpi)\sum_{\alpha=0}^{\infty}\xi_\alpha(\varpi,\tau) + H_d\sum_{\alpha=0}^{\infty}W_\alpha\right)\right\}. \tag{31}$$

Equating the like terms on both sides of equation (20), we finally obtain the general solution of equation (22) given recursively as

$$\begin{aligned} \xi_0(\varpi,\tau) &= \xi(\varpi,0), \\ \xi_1(\varpi,\tau) &= -A^{-1}\left\{\frac{1}{\hbar^\nu} iA\left(-\frac{1}{2}\mathfrak{F}_\varpi \xi_0(\varpi,\tau) + \Theta_d(\varpi)\xi_0(\varpi,\tau) + H_d W_0\right)\right\}, \\ \xi_2(\varpi,\tau) &= -A^{-1}\left\{\frac{1}{\hbar^\nu} iA\left(-\frac{1}{2}\mathfrak{F}_\varpi \xi_1(\varpi,\tau) + \Theta_d(\varpi)\xi_1(\varpi,\tau) + H_d W_1\right)\right\}, \\ \xi_3(\varpi,\tau) &= -A^{-1}\left\{\frac{1}{\hbar^\nu} iA\left(-\frac{1}{2}\mathfrak{F}_\varpi \xi_2(\varpi,\tau) + \Theta_d(\varpi)\xi_2(\varpi,\tau) + H_d W_2\right)\right\}, \\ \xi_{\alpha+1}(\varpi,\tau) &= -A^{-1}\left\{\frac{1}{\hbar^\nu} iA\left(-\frac{1}{2}\mathfrak{F}_\varpi \xi_\alpha(\varpi,\tau) + \Theta_d(\varpi)\xi_\alpha(\varpi,\tau) + H_d W_\alpha\right)\right\}, \\ \xi(\varpi,\tau) &= \xi_0(\varpi,\tau) + \xi_1(\varpi,\tau) + \xi_2(\varpi,\tau) + \cdots, \end{aligned} \tag{32}$$

where $\alpha = 0, 1, 2, \ldots$

The following theorem describes the criteria for the expansion solution to converge.

Theorem 1. *Let M be a Banach space with an appropriate norm . and a series of partial sums $\sum_{\alpha=0}^{\infty} \xi_\alpha(\varpi, \tau)$ defined over it. Assume that the initial guess $w_0 = \xi_0(\varpi, \tau)$ remains inside the ball $B_r(\xi)$ of the solution $\xi(\varpi, \tau)$. Then, the series solution $\sum_{\alpha=0}^{\infty} \xi_\alpha(\varpi, \tau)$ converges if $\exists \sigma > 0$ such that $\xi_{\alpha+1}(\varpi, \tau) \le \sigma \xi_\alpha(\varpi, \tau)$.*

Proof. The following is the description of a sequence of partial sums:

$$\begin{aligned}
\Theta_0 &= \xi_0(\varpi, \tau),\\
\Theta_1 &= \xi_0(\varpi, \tau) + \xi_1(\varpi, \tau),\\
\Theta_2 &= \xi_0(\varpi, \tau) + \xi_1(\varpi, \tau) + \xi_2(\varpi, \tau),\\
\Theta_3 &= \xi_0(\varpi, \tau) + \xi_1(\varpi, \tau) + \xi_2(\varpi, \tau) + \xi_3(\varpi, \tau),\\
&\vdots \quad \vdots \quad \vdots\\
\Theta_\alpha &= \xi_0(\varpi, \tau) + \xi_1(\varpi, \tau) + \xi_2(\varpi, \tau)\\
&\quad + \xi_3(\varpi, \tau) + \cdots + \xi_\alpha(\varpi, \tau).
\end{aligned} \tag{33}$$

Then, we would have to demonstrate that $\{\Theta_\alpha\}_{\alpha=0}^{\infty}$ is a Cauchy sequence in M. To demonstrate this, consider the relationship that

$$\begin{aligned}
\Theta_{\alpha+1} - \Theta_\alpha &= \xi_{\alpha+1}(\varpi, \tau) \le \sigma \xi_\alpha(\varpi, \tau) \le \sigma^2 \xi_{\alpha-1}(\varpi, \tau)\\
&\le \sigma^3 \xi_{\alpha-2}(\varpi, \tau) \le \cdots \sigma^{\alpha+1} \xi_0(\varpi, \tau),
\end{aligned} \tag{34}$$

where $\alpha = 0, 1, 2, 3, \ldots$

For every ℓ, $\alpha \in \mathrm{N}, \alpha \ge \ell$, we have

$$\begin{aligned}
\Theta_\alpha - \Theta_\ell &= (\Theta_\alpha - \Theta_{\alpha-1}) + (\Theta_{\alpha-1} - \Theta_{\alpha-2})\\
&\quad + (\Theta_{\alpha-2} - \Theta_{\alpha-3}) + (\Theta_{\alpha-3} - \Theta_{\alpha-4}) + \sigma^4\\
\xi_{\alpha-3}(\varpi, \tau) &\le \cdots + (\Theta_{\ell+1} - \Theta_\ell).
\end{aligned} \tag{35}$$

We get the following from the triangle inequality:

$$\begin{aligned}
&(\Theta_\alpha - \Theta_{\alpha-1}) + (\Theta_{\alpha-1} - \Theta_{\alpha-2}) + (\Theta_{\alpha-2} - \Theta_{\alpha-3})\\
&\quad + (\Theta_{\alpha-3} - \Theta_{\alpha-4}) + \cdots + (\Theta_{\ell+1} - \Theta_\ell)\\
&\le (\Theta_\alpha - \Theta_{\alpha-1}) + (\Theta_{\alpha-1} - \Theta_{\alpha-2}) + (\Theta_{\alpha-2} - \Theta_{\alpha-3})\\
&\quad + (\Theta_{\alpha-3} - \Theta_{\alpha-4}) + \cdots + (\Theta_{\ell+1} - \Theta_\ell),\\
&\quad (\Theta_\alpha - \Theta_{\alpha-1}) + (\Theta_{\alpha-1} - \Theta_{\alpha-2})\\
&\quad + (\Theta_{\alpha-2} - \Theta_{\alpha-3}) + (\Theta_{\alpha-3} - \Theta_{\alpha-4}) + \cdots +\\
(\Theta_{\ell+1} - \Theta_\ell) &\le \sigma^\alpha \xi_0(\varpi, \tau) + \sigma^{\alpha-1} \xi_0(\varpi, \tau) + \sigma^{\alpha-2} \xi_0(\varpi, \tau) + \cdots\\
&\quad + \sigma^\ell \xi_0(\varpi, \tau) = \left(\frac{1 - \sigma^{\alpha-\ell}}{1 - \sigma}\right) \sigma^{\ell+1} \xi_0(\varpi, \tau).
\end{aligned} \tag{36}$$

As a result, we have the following inequality:

$$\Theta_\alpha - \Theta_\ell \le \left(\frac{1 - \sigma^{\alpha-\ell}}{1 - \sigma}\right) \sigma^{\alpha+1} \xi_0(\varpi, \tau). \tag{37}$$

Demonstrating that the sequence is bounded and we can attain for $0 < \sigma < 1$, that,

$$\lim_{\ell, \alpha \longrightarrow \infty} \Theta_\alpha - \Theta_\ell = 0. \tag{38}$$

As a consequence, the sequence of partial sums of the ATDM is Cauchy and so convergent. □

4. Approximate and Exact Solutions to SDEs with Zero and Nonzero Trapping Potential

In this part, we determined the exact solution to linear and nonlinear time-fractional SDEs with zero and nonzero potential by using the ATDM.

Example 1. We consider the following linear SDE with zero trapping potential:

$$\begin{aligned}
&iD_\tau^\nu \xi(\varpi, \tau) + D_{\varpi\varpi} \xi(\varpi, \tau) = 0,\\
&\qquad 0 < \nu \le 1,\ \tau \ge 0, \varpi \in R,
\end{aligned} \tag{39}$$

with the initial condition:

$$\xi(\varpi, 0) = be^{ia\varpi}. \tag{40}$$

By using the A-T on both sides of equation (39), we get as follows:

$$A\left[iD_\tau^\nu \xi(\varpi, \tau) + D_{\varpi\varpi} \xi(\varpi, \tau)\right] = 0. \tag{41}$$

Using the third part of Lemma 1, equation (41) is transformed as follows:

$$A[\xi(\varpi, \tau)] = \frac{\xi(\varpi, 0)}{\hbar^2} - \frac{1}{\hbar^\nu} D_{\varpi\varpi} A[\xi\varpi, \tau]. \tag{42}$$

By using the inverse A-T, equation (42) becomes as

$$\xi(\varpi, \tau) = A^{-1}\left\{\frac{\xi(\varpi, 0)}{\hbar^2}\right\} - A^{-1}\left\{\frac{1}{\hbar^\nu} D_{\varpi\varpi} A[\xi(\varpi, \tau)]\right\}. \tag{43}$$

By using the procedure of ATDM, as explained in Section 3, the expansion solution of equation (39) can be represented by the expansion form as follows:

$$\xi(\varpi, \tau) = \sum_{\alpha=0}^{\infty} \xi_\alpha(\varpi, \tau). \tag{44}$$

We get as by substituting equation (44) into equation (43).

$$\sum_{\alpha=0}^{\infty} \xi_\alpha(\varpi, \tau) = A^{-1}\left\{\frac{\xi(\varpi, 0)}{\hbar^2}\right\} - A^{-1}\left\{\frac{1}{\hbar^\nu} D_{\varpi\varpi} A\left[\sum_{\alpha=0}^{\infty} \xi_\alpha(\varpi, \tau)\right]\right\}. \tag{45}$$

Using the approach outlined in Section 3, we can get the following from equation (45):

$$\xi_0(\varpi,\tau) = be^{ia\varpi}, \tag{46}$$

$$\xi_{\alpha+1}(\varpi,\tau) = -A^{-1}\left\{\frac{1}{\phi^{\nu}}D_{\varpi\varpi}Q[\xi_\alpha(\varpi,\tau)]\right\}, \quad \alpha = 0, 1, 2, \ldots. \tag{47}$$

By repeating the iteration process in equation (47), we obtain the following results:

$$\begin{aligned}
\xi_1(\varpi,\tau) &= -\frac{i\tau^{\nu}a^2be^{ia\varpi}}{\Gamma(\nu+1)},\\
\xi_2(\varpi,\tau) &= -\frac{\tau^{2\nu}a^4be^{ia\varpi}}{\Gamma(2\nu+1)},\\
\xi_3(\varpi,\tau) &= \frac{i\tau^{3\nu}a^6be^{ia\varpi}}{\Gamma(3\nu+1)},\\
\xi_4(\varpi,\tau) &= \frac{\tau^{4\nu}a^8be^{ia\varpi}}{\Gamma(4\nu+1)},\\
\xi_5(\varpi,\tau) &= -\frac{i\tau^{5\nu}a^{10}be^{ia\varpi}}{\Gamma(5\nu+1)}.
\end{aligned} \tag{48}$$

As a result, we can find the series solution as

$$\begin{aligned}
\xi(\varpi,\tau) = be^{ia\varpi} &- \frac{i\tau^{\nu}a^2be^{ia\varpi}}{\Gamma(\nu+1)} - \frac{\tau^{2\nu}a^4be^{ia\varpi}}{\Gamma(2\nu+1)} + \frac{i\tau^{3\nu}a^6be^{ia\varpi}}{\Gamma(3\nu+1)}\\
&+ \frac{\tau^{4\nu}a^8be^{ia\varpi}}{\Gamma(4\nu+1)} - \frac{i\tau^{5\nu}a^{10}be^{ia\varpi}}{\Gamma(5\nu+1)} + \cdots.
\end{aligned} \tag{49}$$

When we use $\nu = 1$ in equation (49), we get the following precise solution to equation (39).

$$\xi(\varpi,\tau) = be^{ia(\varpi - a\tau)}. \tag{50}$$

Example 2. Consider the following one-dimensional nonlinear SDE with zero trapping potential:

$$\begin{aligned}
iD_{\tau}^{\nu}\xi(\varpi,\tau) + D_{\varpi\varpi}\xi(\varpi,\tau) + 2|\xi(\varpi,\tau)|^2\xi(\varpi,\tau) = 0,\\
0 < \nu \le 1,\ \tau \ge 0, \varpi \in R,
\end{aligned} \tag{51}$$

with the initial condition:

$$\xi(\varpi,0) = e^{i\varpi}. \tag{52}$$

By using A-T on both sides of equation (52), we get as

$$A[\xi(\varpi,\tau)] = \frac{\xi(\varpi,0)}{\hbar^{2-\nu}} + \frac{1}{\hbar^{\nu}}A\left[iD_{\varpi\varpi}\xi(\varpi,\tau)\right] + \frac{1}{\hbar^{\nu}}A\left[2i|\xi(\varpi,\tau)|^2\xi(\varpi,\tau)\right]. \tag{53}$$

By following the process stated in Section 3, we achieve the following result:

$$\begin{aligned}
\xi(\varpi,\tau) = A^{-1}\left\{\frac{e^{i\varpi}}{\hbar^2}\right\} &+ A^{-1}\left\{\frac{1}{\hbar^{\nu}}A\left[iD_{\varpi\varpi}\xi(\varpi,\tau)\right]\right\}\\
&+ A^{-1}\left\{\frac{1}{\hbar^{\nu}}A\left[2i|\xi(\varpi,\tau)|^2\xi(\varpi,\tau)\right]\right\}.
\end{aligned} \tag{54}$$

$$\begin{aligned}
\xi(\varpi,\tau) &= \sum_{\alpha=0}^{\infty}\xi_\alpha(\varpi,\tau),\\
|\xi(\varpi,\tau)|^2\xi(\varpi,\tau) &= \aleph(\xi(\varpi,\tau)),\\
\aleph(\xi(\varpi,\tau)) &= \sum_{\alpha=0}^{\infty}Q_\alpha(\xi_0,\xi_1,\xi_2,\ldots),\\
W_0 &= \xi_0^2(\varpi,\tau)\overline{\xi(\varpi,\tau)},\\
W_1 &= \xi_0^2(\varpi,\tau)\overline{\xi_1(\varpi,\tau)}\\
&\quad + 2\xi_0(\varpi,\tau)\xi_1(\varpi,\tau)\overline{\xi_0(\varpi,\tau)},\\
W_2 &= \xi_1^2(\varpi,\tau)\overline{\xi_0(\varpi,\tau)}\\
&\quad + 2\xi_0(\varpi,\tau)\xi_2(\varpi,\tau)\overline{\xi_0(\varpi,\tau)}\\
&\quad + 2\xi_0(\varpi,\tau)\xi_1(\varpi,\tau)\overline{\xi_1(\varpi,\tau)}\\
&\quad + \xi_0^2(\varpi,\tau)\overline{\xi_0(\varpi,\tau)}.
\end{aligned} \tag{55}$$

By using equation (55) in equation (54), we obtain as follows:

$$\begin{aligned}
\sum_{\alpha=0}^{\infty}\xi_\alpha(\varpi,\tau) = A^{-1}\left\{\frac{e^{i\varpi}}{\hbar^2}\right\} &+ A^{-1}\left\{\frac{1}{\hbar^{\nu}}A\left[iD_{\varpi\varpi}\sum_{\alpha=0}^{\infty}\xi_\alpha(\varpi,\tau)\right]\right\}\\
&+ A^{-1}\left\{\frac{1}{\hbar^{\nu}}A\left[2i\sum_{\alpha=0}^{\infty}Q_\alpha\right]\right\}.
\end{aligned} \tag{56}$$

By following the process stated in Section 3, we achieve the following result:

$$\begin{aligned}
\xi_0(\varpi,\tau) &= e^{i\varpi},\\
\xi_1(\varpi,\tau) &= \frac{e^{i\varpi}(i\tau^{\nu})^1}{\Gamma(\nu+1)},\\
\xi_2(\varpi,\tau) &= \frac{e^{i\varpi}(i\tau^{\nu})^2}{\Gamma(2\nu+1)},\\
\xi_3(\varpi,\tau) &= \frac{e^{i\varpi}(i\tau^{\nu})^3}{\Gamma(3\nu+1)},\\
\xi_4(\varpi,\tau) &= \frac{e^{i\varpi}(i\tau^{\nu})^4}{\Gamma(4\nu+1)},\\
\xi_5(\varpi,\tau) &= \frac{e^{i\varpi}(i\tau^{\nu})^5}{\Gamma(5\nu+1)}.
\end{aligned} \tag{57}$$

As a result, we get the following solution in series form for equation (51).

$$\xi(\varpi,\tau)=e^{i\varpi}+\frac{e^{i\varpi}(i\tau^{\nu})^{1}}{\Gamma(\nu+1)}+\frac{e^{i\varpi}(i\tau^{\nu})^{2}}{\Gamma(2\nu+1)}+\frac{e^{i\varpi}(i\tau^{\nu})^{3}}{\Gamma(3\nu+1)}+\frac{e^{i\varpi}(9i\tau^{\nu})^{4}}{\Gamma(4\nu+1)}+\frac{e^{i\varpi}(i\tau^{\nu})^{5}}{\Gamma(5\nu+1)}+\cdots. \tag{58}$$

When we use $\nu=1$ in equation (58), we get the following precise solution to equation (51).

$$\xi(\varpi,\tau)=e^{i(\varpi+\tau)}. \tag{59}$$

Example 3. Consider the following one-dimensional nonlinear SDE with trapping potential:

$$D_{\tau}^{\nu}\xi(\varpi,\tau)=-i\left(-\frac{1}{2}D_{\varpi}\xi(\varpi,\tau)+\cos^{2}\varpi\xi(\varpi,\tau)+|\xi(\varpi,\tau)|^{2}\xi(\varpi,\tau)\right),\quad 0<\nu\le 1,\ \tau\ge 0,\varpi\in R. \tag{60}$$

with the initial condition:

$$\xi(\varpi,0)=\sin\varpi. \tag{61}$$

By using the A-T on both sides of equation (69), we obtain as follows:

$$A\left[D_{\tau}^{\nu}\xi(\varpi,\tau)\right]=A\left[-i\left(-\frac{1}{2}D_{\varpi}\xi(\varpi,\tau)+\cos^{2}\varpi\xi(\varpi,\tau)+|\xi(\varpi,\tau)|^{2}\xi(\varpi,\tau)\right)\right]. \tag{62}$$

Using the third part of Lemma 1, equation (62) is transformed as follows:

$$A[\xi(\varpi,\tau)]=\frac{\xi(\varpi,0)}{\hbar^{2}}+\frac{1}{\hbar^{\nu}}A\left[-i\left(-\frac{1}{2}D_{\varpi}\xi(\varpi,\tau)+\cos^{2}\varpi\xi(\varpi,\tau)+|\xi(\varpi,\tau)|^{2}\xi(\varpi,\tau)\right)\right]. \tag{63}$$

On both sides of equation (63), consider the inverse of the A-T.

$$\xi(\varpi,\tau)=A^{-1}\left\{\frac{\xi(\varpi,0)}{\hbar^{2}}\right\}+A^{-1}\left\{\frac{1}{\hbar^{\nu}}A\left[-i\left(-\frac{1}{2}D_{\varpi}\xi(\varpi,\tau)+\cos^{2}\varpi\xi(\varpi,\tau)+|\xi(\varpi,\tau)|^{2}\xi(\varpi,\tau)\right)\right]\right\}. \tag{64}$$

By following the process stated in Section 3, we achieve the following result:

$$\xi(\varpi,\tau)=\sum_{\alpha=0}^{\infty}\xi_{\alpha}(\varpi,\tau),\qquad Q(\xi(\varpi,\tau))=|\xi(\varpi,\tau)|^{2}\xi(\varpi,\tau)=\sum_{\alpha=0}^{\infty}W_{\alpha}. \tag{65}$$

Using equation (65) in equation (64), we get as follows:

$$\sum_{\alpha=0}^{\infty}\xi_{\alpha}(\varpi,\tau)=A^{-1}\left\{\frac{\xi(\varpi,0)}{\hbar^{2}}\right\}+A^{-1}\left\{\frac{1}{\hbar^{\nu}}A\left[-i\left(-\frac{1}{2}D_{\varpi}\sum_{\alpha=0}^{\infty}\xi_{\alpha}(\varpi,\tau)+\cos^{2}\varpi\sum_{\alpha=0}^{\infty}\xi_{\alpha}(\varpi,\tau)+\sum_{\alpha=0}^{\infty}W_{\alpha}\right)\right]\right\}. \tag{66}$$

By equating the like terms on both sides of equation (66), we get as follows:

$$\xi_{0}(\varpi,\tau)=A^{-1}\left\{\frac{\xi(\varpi,0)}{\hbar^{2}}\right\},\qquad \xi_{\alpha+1}(\varpi,\tau)=A^{-1}\left\{\frac{1}{\hbar^{\nu}}A\left[-i\left(-\frac{1}{2}D_{\varpi}\xi_{\alpha}(\varpi,\tau)+\cos^{2}\varpi\xi_{\alpha}(\varpi,\tau)+W_{\alpha}\right)\right]\right\}. \tag{67}$$

The following results are obtained from equation (67) using the iteration procedure stated in Section 3.

$$\begin{aligned}\xi_{0}(\varpi,\tau)&=\sin\varpi,\\ \xi_{1}(\varpi,\tau)&=-\frac{3i\tau^{\nu}}{2\Gamma(\nu+1)}\sin\varpi,\\ \xi_{2}(\varpi,\tau)&=-\frac{9\tau^{2\nu}}{4\Gamma(2\nu+1)}\sin\varpi,\\ \xi_{3}(\varpi,\tau)&=\frac{27i\tau^{3\nu}}{8\Gamma(3\nu+1)}\sin\varpi,\\ \xi_{4}(\varpi,\tau)&=\frac{81\tau^{4\nu}}{16\Gamma(4\nu+1)}\sin\varpi,\\ \xi_{5}(\varpi,\tau)&=-\frac{243i\tau^{5\nu}}{32\Gamma(5\nu+1)}\sin\varpi.\end{aligned} \tag{68}$$

As a result, we get the following solution in series form for equation (60).

$$\xi(\varpi,\tau)=\sin\varpi-\frac{3i\tau^{\nu}}{2\Gamma(\nu+1)}\sin\varpi-\frac{9\tau^{2\nu}}{4\Gamma(2\nu+1)}\sin\varpi+\frac{27i\tau^{3\nu}}{8\Gamma(3\nu+1)}\sin\varpi+\frac{81\tau^{4\nu}}{16\Gamma(4\nu+1)}\sin\varpi-\frac{243i\tau^{5\nu}}{32\Gamma(5\nu+1)}\sin\varpi+\cdots. \tag{69}$$

When we use $\nu = 1$ in equation (69), we get the following precise solution to equation (60).

$$\xi(\varpi, \tau) = \sin \varpi e^{-(3i/2)\tau}. \tag{70}$$

Example 4. Consider the nonlinear three-dimensional SDE with trapping potential:

$$D_\tau^\nu \xi(\varpi, \beta, \mu, \tau) = -i\left(-\frac{1}{2}\left(\frac{\partial^2}{\partial \varpi^2} + \frac{\partial^2}{\partial \beta^2} + \frac{\partial^2}{\partial \mu^2}\right)\xi(\varpi, \beta, \mu, \tau) + K(\varpi, \beta, \mu)\xi(\varpi, \beta, \mu, \tau) + |\xi(\varpi, \beta, \mu, \tau)|^2 \xi(\varpi, \beta, \mu, \tau)\right), \tag{71}$$

where $0 < \nu \le 1$, $\tau \ge 0, \varpi, \beta, \mu \in R \times R \times R$, and $K(\varpi, \beta, \mu) = 1 - \sin^2 \varpi \sin^2 \beta \sin^2 \mu$, with the initial condition:

$$\xi(\varpi, \beta, \mu, 0) = \sin \varpi \sin \beta \sin \mu. \tag{72}$$

Using the A-T on equation (71), we get:

$$A\left[D_\tau^\nu \xi(\varpi, \beta, \mu, \tau)\right] = A\left[-i\left(-\frac{1}{2}\left(\frac{\partial^2}{\partial \varpi^2} + \frac{\partial^2}{\partial \beta^2} + \frac{\partial^2}{\partial \mu^2}\right)\xi(\varpi, \tau) + K(\varpi, \beta, \mu)\xi(\varpi, \beta, \mu, \tau) + |\xi(\varpi, \beta, \mu, \tau)|^2 \xi(\varpi, \beta, \mu, \tau)\right)\right]. \tag{73}$$

Using the third part of Lemma 1, equation (73) is transformed as follows:

$$A[\xi(\varpi, \beta, \mu, \tau)] = \frac{\xi(\varpi, \beta, \mu, 0)}{\hbar^2} + \frac{1}{\hbar^\nu} A\left[-i\left(-\frac{1}{2}\left(\frac{\partial^2}{\partial \varpi^2} + \frac{\partial^2}{\partial \beta^2} + \frac{\partial^2}{\partial \mu^2}\right)\xi(\varpi, \beta, \mu, \tau) + K(\varpi, \beta, \mu)\xi(\varpi, \beta, \mu, \tau) + |\xi(\varpi, \beta, \mu, \tau)|^2 \xi(\varpi, \beta, \mu, \tau)\right)\right]. \tag{74}$$

On both sides of equation (74), consider the inverse of the A-T.

$$\xi(\varpi, \beta, \mu, \tau) = A^{-1}\left\{\frac{\xi(\varpi, \beta, \mu, 0)}{\hbar^2}\right\} + A^{-1}\left\{\frac{1}{\hbar^\nu} A\left[-i\left(-\left(\frac{\partial^2}{\partial \varpi^2} + \frac{\partial^2}{\partial \beta^2} + \frac{\partial^2}{\partial \mu^2}\right)\frac{1}{2}\xi(\varpi, \beta, \mu, \tau) + K(\varpi, \beta, \mu)\xi(\varpi, \beta, \mu, \tau) + |\xi(\varpi, \beta, \mu, \tau)|^2 \xi(\varpi, \beta, \mu, \tau)\right)\right]\right\}. \tag{75}$$

By following the process stated in Section 3, we achieve the following result:

$$\begin{aligned} \xi(\varpi, \beta, \mu, \tau) &= \sum_{\alpha=0}^{\infty} \xi_\alpha(\varpi, \beta, \mu, \tau), \\ Q(\xi(\varpi, \beta, \mu, \tau)) &= |\xi(\varpi, \beta, \mu, \tau)|^2 \xi(\varpi, \beta, \mu, \tau) = \sum_{\alpha=0}^{\infty} W_\alpha. \end{aligned} \tag{76}$$

Using equation (76) in equation (75), we get as follows:

$$\sum_{\alpha=0}^{\infty} \xi_\alpha(\varpi, \beta, \mu, \tau) = A^{-1}\left\{\frac{\xi(\varpi, \beta, \mu, 0)}{\hbar^2}\right\} + A^{-1}\left\{\frac{1}{\hbar^\nu} A\left[-i\left(-\frac{1}{2}\left(\frac{\partial^2}{\partial \varpi^2} + \frac{\partial^2}{\partial \beta^2} + \frac{\partial^2}{\partial \mu^2}\right)\sum_{\alpha=0}^{\infty} \xi_\alpha(\varpi, \beta, \mu, \tau) + K(\varpi, \beta, \mu)\sum_{\alpha=0}^{\infty} \xi_\alpha(\varpi, \beta, \mu, \tau) + \sum_{\alpha=0}^{\infty} W_\alpha\right)\right]\right\}. \tag{77}$$

By equating the like terms on both sides of equation (77), we get as follows:

$$\xi_0(\varpi,\beta,\mu,\tau) = A^{-1}\left\{\frac{\xi(\varpi,\beta,\mu,0)}{\hbar^2}\right\},$$
$$\xi_{\alpha+1}(\varpi,\beta,\mu,\tau) = A^{-1}\left\{\frac{1}{\hbar^{\nu}}A\left[-i\left(-\frac{1}{2}\left(\frac{\partial^2}{\partial\varpi^2}+\frac{\partial^2}{\partial\beta^2}+\frac{\partial^2}{\partial\mu^2}\right)\xi_\alpha(\varpi,\beta,\mu,\tau)+K(\varpi,\beta,\mu)\xi_\alpha(\varpi,\beta,\mu,\tau)+W_\alpha\right)\right]\right\}. \tag{78}$$

The following results are obtained from equation (78) using the iteration procedure stated in Section 3.

$$\begin{aligned}
\xi_0(\varpi,\beta,\mu,\tau) &= \sin\varpi\sin\beta\sin\mu,\\
\xi_1(\varpi,\beta,\mu,\tau) &= -\frac{5i\tau^{\nu}}{2\Gamma(\nu+1)}\sin\varpi\sin\beta\sin\mu,\\
\xi_2(\varpi,\beta,\mu,\tau) &= \frac{25i^2\tau^{2\nu}}{4\Gamma(2\nu+1)}\sin\varpi\sin\beta\sin\mu,\\
\xi_3(\varpi,\beta,\mu,\tau) &= -\frac{125i^3\tau^{3\nu}}{8\Gamma(3\nu+1)}\sin\varpi\sin\beta\sin\mu,\\
\xi_4(\varpi,\beta,\mu,\tau) &= \frac{625i^4\tau^{4\nu}}{16\Gamma(4\nu+1)}\sin\varpi\sin\beta\sin\mu,\\
\xi_5(\varpi,\beta,\mu,\tau) &= -\frac{3125i^5\tau^{5\nu}}{32\Gamma(5\nu+1)}\sin\varpi\sin\beta\sin\mu.
\end{aligned} \tag{79}$$

As a result, we get the following solution in series form for equation (78).

$$\begin{aligned}
\xi(\varpi,\beta,\mu,\tau) = {} & \sin\varpi\sin\beta\sin\mu - \frac{5i\tau^{\nu}}{2\Gamma(\nu+1)}\sin\varpi\sin\beta\sin\mu\\
& + \frac{25i^2\tau^{2\nu}}{4\Gamma(2\nu+1)}\sin\varpi\sin\beta\sin\mu\\
& - \frac{125i^3\tau^{3\nu}}{8\Gamma(3\nu+1)}\sin\varpi\sin\beta\sin\mu\\
& + \frac{625i^4\tau^{4\nu}}{16\Gamma(4\nu+1)}\sin\varpi\sin\beta\sin\mu\\
& - \frac{3125i^5\tau^{5\nu}}{32\Gamma(5\nu+1)}\sin\varpi\sin\beta\sin\mu+\cdots.
\end{aligned} \tag{80}$$

When we use $\nu = 1$ in equation (80), we get the following precise solution to equation (78).

$$\xi(\varpi,\beta,\mu,\tau) = \sin\varpi\sin\beta\sin\mu e^{-(i5/2)\tau}. \tag{81}$$

5. Numerical Simulation and Discussion

In this section, we discuss and evaluate the graphic and numerical results of the approximate and exact solutions to the models discussed in Examples 1–4. Figures 1–8 represent the 2D graphs of the 5th approximate solution obtained by ATDM at $\nu = 0.6, 0.7, 0.8, 0.9, 1.0$ and the exact solution. These figures show that the approximate solutions obtained by the ATDM approach the exact solutions. The approximate result corresponds with the precise result at $\nu = 1$, and this proves the effectiveness and precision of the suggested method. Figures 9–16 demonstrate the 2D graph of absolute error over the 5th term, with approximate and exact solutions to Examples 1–4. As for the figure, approximate and exact solutions are in very good agreement. Tables 1–4 show comparisons of the absolute error of the 5th approximate solution obtained by ATDM of Examples 1–4 at $\nu = 1$ with the absolute error of approximate solutions obtained by FRDTM [42], HPM [35], and HAM [43]. The results obtained from the suggested method are extremely similar to those obtained by FRDTM, HPM, and HAM. The convergence of the approximate solution to the exact solution for Examples 1–4 has been shown numerically as in Tables 5–12. The results show that the proposed method is a useful and efficient algorithm for solving certain classes of fractional-order differential equations with fewer calculations and iteration steps. The 3D graphs of these solutions are also sketched to show the behavior of the exact solutions in Figures 17–24.

The following 2D graphs show the real and imaginary parts of approximate and exact solutions to Example 1:

Figures 1 and 2 show the behavior of real imaginary in the interval $\tau \in [0, 1]$ between the 5th step iteration approximate and exact solutions of equation (39) at several values of ν when $\varpi = 0.05$, $a = 1$ and $b = 1$. The approximate result corresponds with the precise result at $\nu = 1$ and this proves the effectiveness and precision of the suggested method.

The graphs of absolute error for the real and imaginary parts of the 5th approximation and exact solutions to Example 1 are as follows:

Figures 9 and 10 demonstrate the 2D graph of real and imaginary parts of absolute error in the intervals $\tau \in [0, 1]$ when $\varpi = 0.05$, $a = 1$, and $b = 1$ are over the 5th terms, approximate and exact solutions of equation (39) at $\nu = 1$. As

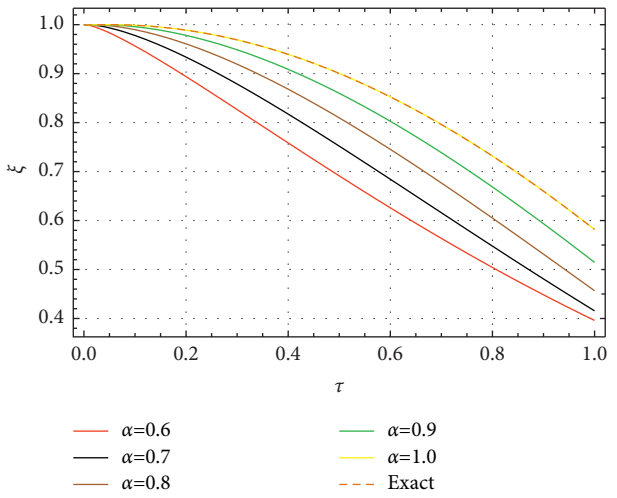

Figure 1: The approximate and exact solutions to the real part of Example 1.

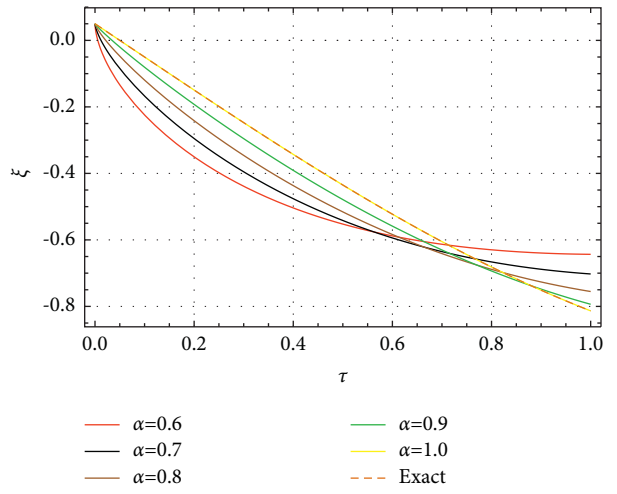

Figure 2: The approximate and exact solutions to the imaginary part of Example 1.

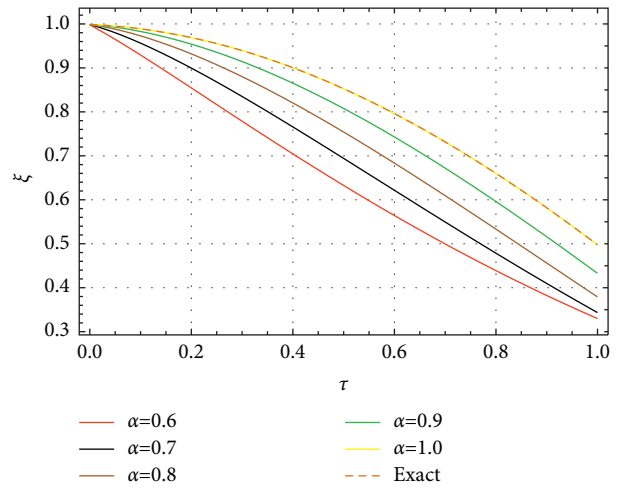

Figure 3: The approximate and exact solutions to the real part of Example 2.

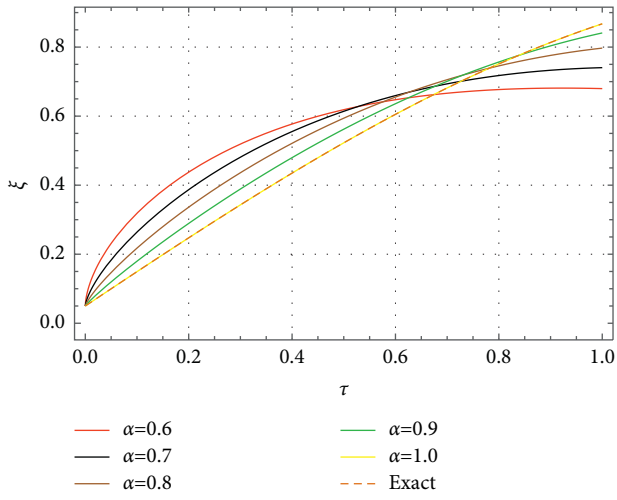

Figure 4: The approximate and exact solutions to the imaginary part of Example 2.

for the figures, approximate and exact solutions are in very good agreement.

The accuracy and capability of the numerical method can be determined using error functions. To demonstrate the accuracy and capability of the ATDM, we used recurrence and absolute error functions.

Table 1 shows comparisons of the real and imaginary parts of the absolute error of the 5th approximate solution obtained by ATDM in Example 1 at $\nu = 1$ with the absolute error of approximate solutions obtained by FRDTM [42]. The results obtained from the suggested method are extremely similar to those obtained by FRDTM.

The recurrence error $|\xi^5(\varpi, \tau) - \xi^4(\varpi, \tau)|$ between the 5th and 4th approximate solutions of the real part with different values of ν, when $\varpi = 0.05$, $a = 1$, and $b = 1$ in Example 1 are presented as follows:

The recurrence error $|\xi^5(\varpi, \tau) - \xi^4(\varpi, \tau)|$ between the 5th and 4th approximate solutions of the imaginary part with different values of ν, when $\varpi = 0.05$, $a = 1$, and $b = 1$ in Example 1 are presented as follows:

The convergence of the ATDM of real and imaginary of the approximate solution to the exact solution for equation (39) has been shown numerically as in Tables 5 and 6. The results show that the current technique is a useful and efficient algorithm for solving fractional-order differential equations with fewer calculations and iteration steps.

The following are 3D graphs for the real and imaginary parts of the exact solution to Example 1:

The real and imaginary parts of the exact solution equation (39) at $\nu = 1$ are shown in Figures 17 and 18 respectively in the intervals $\tau \in [0, 2]$, $\varpi \in [-2\pi, 2\pi]$ with $a = 1$ and $b = 1$.

The following 2D graphs show the real and imaginary parts of approximate and exact solutions to Example 2:

Figures 3 and 4 show the behavior of real and imaginary parts in the interval $\tau \in [0, 1]$ between the 5th step iteration

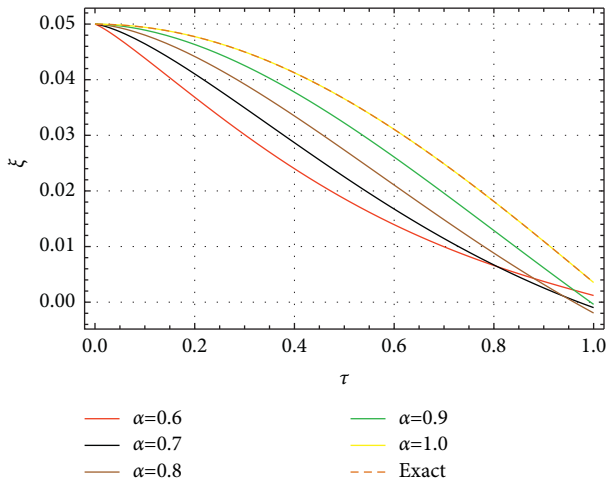

Figure 5: The approximate and exact solutions to the real part of Example 3.

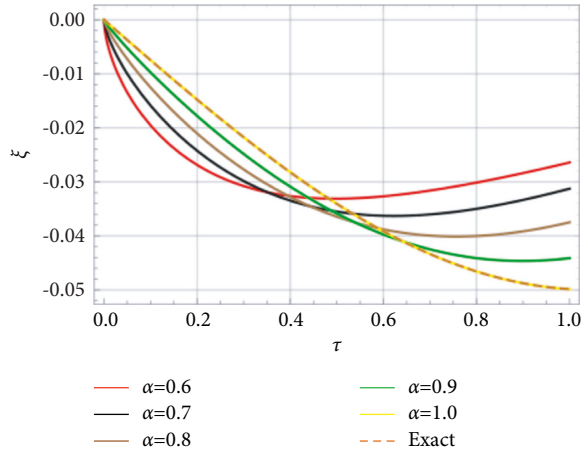

Figure 6: The approximate and exact solutions to the imaginary part of Example 3.

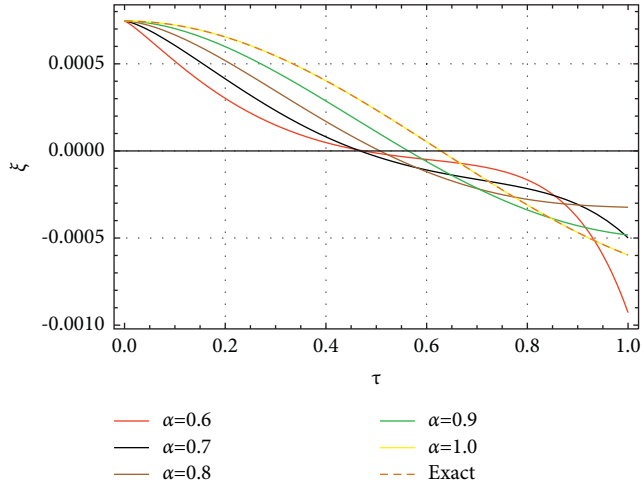

Figure 7: The approximate and exact solutions to the real part of Example 4.

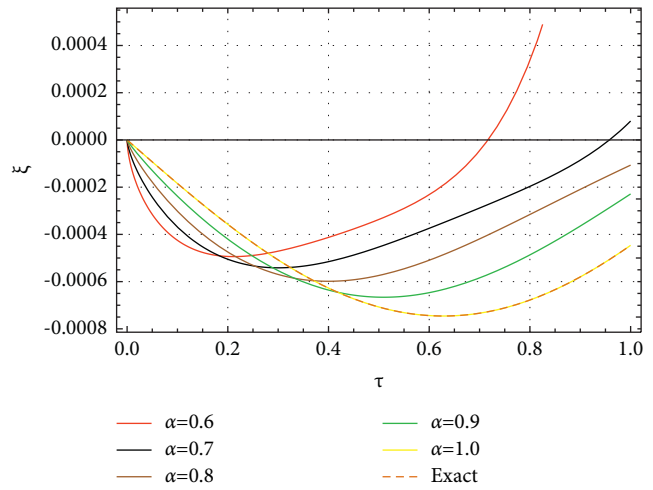

Figure 8: The approximate and exact solutions to the imaginary part of Example 4.

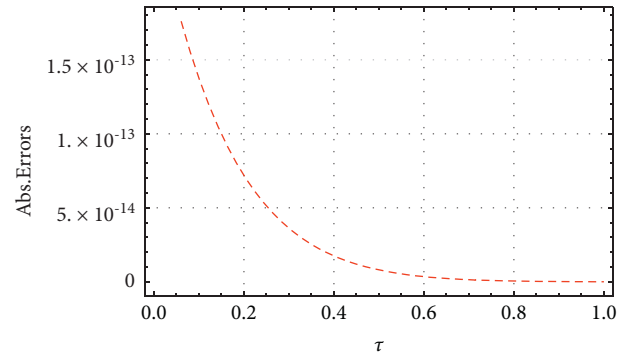

Figure 9: The absolute error for the real part of Example 1.

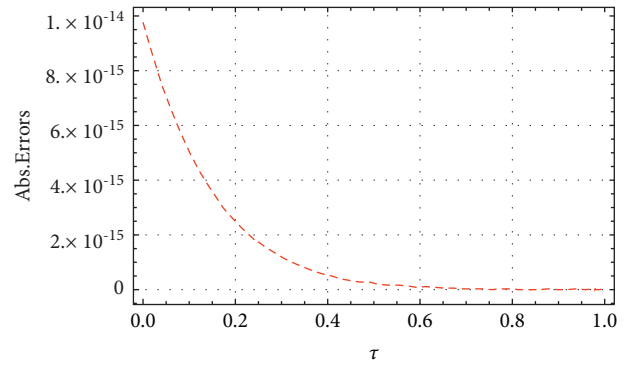

Figure 10: The absolute error for the imaginary part of Example 1.

approximate and exact solutions of equation (51) at several values of ν when $\varpi = 0.05$. The approximate result corresponds with the precise result at $\nu = 1$, and this proves the effectiveness and precision of the suggested method.

The graphs of absolute error for the real and imaginary parts of the 5th approximation and exact solutions to Example 2 are as follows:

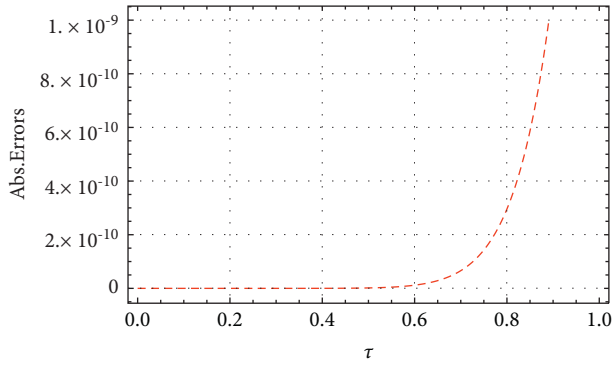

Figure 11: The absolute error for the real part of Example 2.

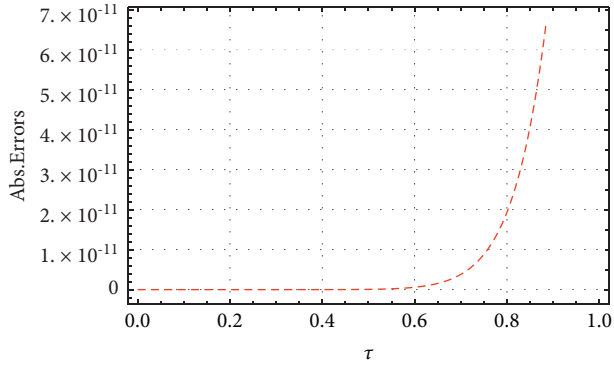

Figure 12: The absolute error for the imaginary part of Example 2.

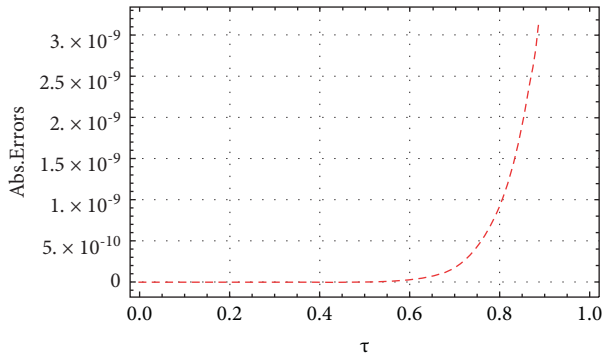

Figure 13: The absolute error for the real part of Example 3.

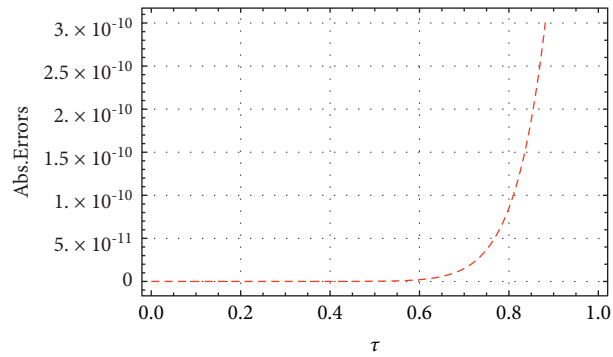

Figure 14: The absolute error for the imaginary part of Example 3.

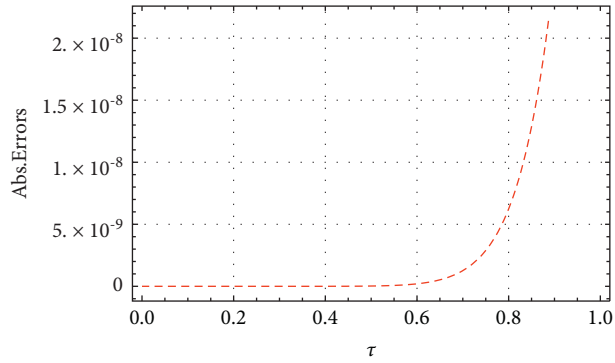

Figure 15: The absolute error for the real part of Example 4.

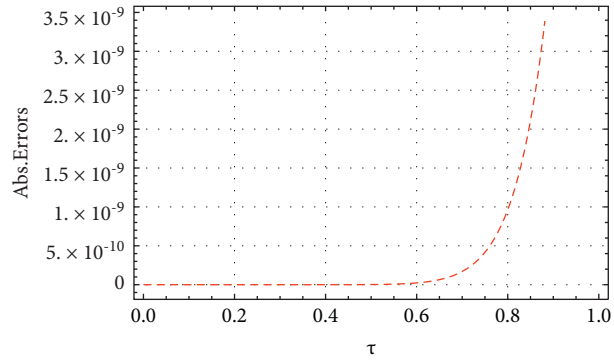

Figure 16: The absolute error for the imaginary part of Example 4.

Figures 11 and 12 demonstrate the 2D graph of real and imaginary parts of absolute error in the intervals $\tau \in [0, 1]$ when $\varpi = 0.05$ are over the 5th terms approximate and exact solutions of equation (51) at $\nu = 1$. As for the figures, approximate and precise solutions are in very good agreement.

Table 2 shows comparisons of the real and imaginary parts of absolute error of the 5th approximate solution obtained by ATDM of Example 2 at $\nu = 1$ with the absolute error of approximate solutions obtained by FRDTM [42]. The results obtained from the suggested method are extremely similar to those obtained by FRDTM.

The recurrence error $|\xi^5(\varpi, \tau) - \xi^4(\varpi, \tau)|$ between the 5th and 4th approximate solutions of the real part with different values of ν, when $\varpi = 0.05$ in Example 2 are presented as follows:

The recurrence error $|\xi^5(\varpi, \tau) - \xi^4(\varpi, \tau)|$ between the 5th and 4th approximate solutions of the imaginary part with different values of ν, when $\varpi = 0.05$ in Example 2 are presented as follows:

The convergence of the ATDM of real and imaginary of the approximate solution to the exact solution for equation (51) has been shown numerically as in Tables 7 and 8. The results show that the current technique is a useful and

Table 2: The absolute error in ATDM and FRDTM for Example 2 at $\nu = 2$.

τ	Real part [ATDM] Abs. error	Img. part [ATDM] Abs. error	Real part [FRDTM] Abs. error	Img. part [FRTDM] Abs. error
0.2	0	$2.775557561562891 \times 10^{-17}$	0	$2.775557561562891 \times 10^{-17}$
0.4	$3.508304757815494 \times 10^{-14}$	$2.886579864025407 \times 10^{-15}$	$3.508304757815494 \times 10^{-14}$	$2.886579864025407 \times 10^{-15}$
0.6	$4.519384866341625 \times 10^{-12}$	$4.35984581770299 \times 10^{-13}$	$4.519384866341625 \times 10^{-12}$	$4.35984581770299 \times 10^{-13}$
0.8	$1.423423601210061 \times 10^{-10}$	$1.593580822856211 \times 10^{-11}$	$1.423423601210061 \times 10^{-10}$	$1.593580822856211 \times 10^{-11}$
1.0	$2.065669746365017 \times 10^{-9}$	$2.633981921462691 \times 10^{-10}$	$2.065669746365017 \times 10^{-9}$	$2.633981921462691 \times 10^{-10}$

Table 3: The absolute error in ATDM and HPM for Example 3 at $\nu = 1$.

τ	Real part [ATDM] Abs. error	Img. part [ATDM] Abs. error	Real part [HPM] Abs. error	Img. part [HPM] Abs. error
0.2	$5.551115123125783 \times 10^{-17}$	0	$5.551115123125783 \times 10^{-17}$	0
0.4	$2.266797860528413 \times 10^{-13}$	$1.047079090099600 \times 10^{-14}$	$2.266797860528413 \times 10^{-13}$	$1.047079090099600 \times 10^{-14}$
0.6	$2.933806669824790 \times 10^{-11}$	$2.032304879939772 \times 10^{-12}$	$2.933806669824790 \times 10^{-11}$	$2.032304879939772 \times 10^{-12}$
0.8	$9.229918426778560 \times 10^{-10}$	$8.528888012504510 \times 10^{-11}$	$9.229918426778560 \times 10^{-10}$	$8.528888012504510 \times 10^{-11}$
1.0	$1.337196644298627 \times 10^{-8}$	$1.545451835949229 \times 10^{-9}$	$1.337196644298627 \times 10^{-8}$	$1.5454518359492290 \times 10^{-9}$

Table 4: The absolute error in ATDM and HAM for Example 4 at $\nu = 1$.

τ	Real part [ATDM] Abs. error	Img. part [ATDM] Abs. error	Real part [HAM] Abs. error	Img. part [HAM] Abs. error
0.2	$3.794707603699265 \times 10^{-16}$	$1.463672932855431 \times 10^{-17}$	$3.794707603699265 \times 10^{-16}$	$1.463672932855431 \times 10^{-17}$
0.4	$1.548127132131732 \times 10^{-12}$	$1.191737680761306 \times 10^{-13}$	$1.548127132131732 \times 10^{-12}$	$1.191737680761306 \times 10^{-13}$
0.6	$1.994952888051838 \times 10^{-10}$	$2.305647122877174 \times 10^{-11}$	$1.994952888051838 \times 10^{-10}$	$2.305647122877174 \times 10^{-11}$
0.8	$6.238188888683330 \times 10^{-9}$	$9.625127946185849 \times 10^{-10}$	$6.238188888683330 \times 10^{-9}$	$9.625127946185849 \times 10^{-10}$
1.0	$8.967831111224030 \times 10^{-8}$	$1.732387384885186 \times 10^{-8}$	$8.967831111224030 \times 10^{-8}$	$1.732387384885186 \times 10^{-8}$

Table 5: The recurrence error of the 5th approximate solution of the real part in Example 1.

τ	$\nu = 0.7$	$\nu = 0.8$	$\nu = 0.9$	$\nu = 1.0$
0.1	$1.9863230258832510 \times 10^{-11}$	$2.480476538225475 \times 10^{-13}$	$2.754480547804426 \times 10^{-15}$	$2.753540058639898 \times 10^{-17}$
0.2	$2.5462310564404910 \times 10^{-9}$	$6.356503419032404 \times 10^{-11}$	$1.41126628375623 \times 10^{-12}$	$2.820907153618413 \times 10^{-14}$
0.3	$4.3559264601363860 \times 10^{-8}$	$1.630598080005387 \times 10^{-9}$	$5.428928326273314 \times 10^{-11}$	$1.6274165548755540 \times 10^{-12}$
0.4	$3.2669475564040040 \times 10^{-7}$	$1.630154704745158 \times 10^{-8}$	$7.234972435809250 \times 10^{-10}$	$2.8912347348589850 \times 10^{-11}$
0.5	$1.5594317330665020 \times 10^{-6}$	$9.724388066839424 \times 10^{-8}$	$5.393791208135125 \times 10^{-9}$	$2.6938949149435820 \times 10^{-10}$
0.6	$5.5932228619978110 \times 10^{-6}$	$4.184575219876433 \times 10^{-7}$	$2.784754999984136 \times 10^{-8}$	$1.6687458133498650 \times 10^{-9}$
0.7	$1.6470066797307933 \times 10^{-5}$	$1.437319768581204 \times 10^{-6}$	$1.115745763781643 \times 10^{-7}$	$7.7992900939752010 \times 10^{-9}$
0.8	$4.1978532985731196 \times 10^{-5}$	$4.186076646645796 \times 10^{-6}$	$3.713180897405904 \times 10^{-7}$	$2.9660020264616400 \times 10^{-8}$
0.9	$9.5822726035593689 \times 10^{-5}$	$1.0748242434163506 \times 10^{-6}$	$1.072429735204339 \times 10^{-6}$	$9.6359264875560130 \times 10^{-8}$
1.0	$2.0050812724929500 \times 10^{-4}$	$2.498621265629671 4 \times 10^{-5}$	$2.769704199336456 \times 10^{-6}$	$2.7648088107301450 \times 10^{-7}$

Table 6: The recurrence error of the 5th approximate solution of the imaginary part in Example 1.

τ	$\nu = 0.7$	$\nu = 0.8$	$\nu = 0.9$	$\nu = 1.0$
0.1	$5.729282854280857 \times 10^{-14}$	$5.566602532673186 \times 10^{-15}$	$9.391428658269753 \times 10^{-17}$	$1.127083924407682 \times 10^{-18}$
0.2	$6.735588070529998 \times 10^{-13}$	$1.29434773662193 \times 10^{-13}$	$2.86554558790132 \times 10^{-14}$	$8.979209489138208 \times 10^{-16}$
0.3	$2.240327760588405 \times 10^{-9}$	$2.657335380224294 \times 10^{-11}$	$3.928763432275554 \times 10^{-13}$	$3.7004114535955 \times 10^{-14}$
0.4	$2.415220588436187 \times 10^{-8}$	$5.443488739768476 \times 10^{-10}$	$3.891048192098205 \times 10^{-12}$	$3.947468488238387 \times 10^{-13}$
0.5	$1.477344106931362 \times 10^{-7}$	$4.825025026815447 \times 10^{-9}$	$9.526894455781187 \times 10^{-11}$	$1.232929037808270 \times 10^{-12}$
0.6	$6.392078149330569 \times 10^{-7}$	$2.727397229393246 \times 10^{-8}$	$8.267292729705227 \times 10^{-10}$	$7.495149197961302 \times 10^{-12}$
0.7	$2.187803743850105 \times 10^{-6}$	$1.152748324472957 \times 10^{-7}$	$4.630213360876863 \times 10^{-9}$	$1.0569208657930970 \times 10^{-10}$
0.8	$6.320873774992085 \times 10^{-6}$	$3.96750649205628 \times 10^{-7}$	$1.972744306783386 \times 10^{-8}$	$6.7041439426968450 \times 10^{-10}$
0.9	$1.606257206934282 \times 10^{-5}$	$1.171284786793358 \times 10^{-6}$	$6.92782295622906 \times 10^{-8}$	$3.0494721017930660 \times 10^{-9}$
1.0	$3.691229597776269 \times 10^{-5}$	$3.069260602197251 \times 10^{-6}$	$2.103049742344222 \times 10^{-7}$	$1.1247880551985750 \times 10^{-8}$

Table 7: The recurrence error of the the approximate solution of the real part in Example 2.

τ	$\nu = 0.7$	$\nu = 0.8$	$\nu = 0.9$	$\nu = 1.0$
0.1	$1.976971658223765 \times 10^{-11}$	$2.473641816908283 \times 10^{-13}$	$2.750095402344202 \times 10^{-15}$	$2.751035891508731 \times 10^{-17}$
0.2	$2.52678613921649 \times 10^{-9}$	$6.326039570110015 \times 10^{-11}$	$1.407076602719864 \times 10^{-12}$	$2.815778619333783 \times 10^{-14}$
0.3	$4.311799014005643 \times 10^{-8}$	$1.619798972797868 \times 10^{-9}$	$5.405728516404219 \times 10^{-11}$	$1.622980497927706 \times 10^{-12}$
0.4	$3.226514454036917 \times 10^{-7}$	$1.616576300475306 \times 10^{-8}$	$7.19494314294836 \times 10^{-10}$	$2.880731496644064 \times 10^{-11}$
0.5	$1.536892238892099 \times 10^{-6}$	$9.627636757901811 \times 10^{-8}$	$5.357333694498901 \times 10^{-9}$	$2.681667536373432 \times 10^{-10}$
0.6	$5.501465744903981 \times 10^{-6}$	$4.136441235299919 \times 10^{-7}$	$2.762589303466765 \times 10^{-8}$	$1.659660768720673 \times 10^{-9}$
0.7	$1.616936914302743 \times 10^{-5}$	$1.418630876198142 \times 10^{-6}$	$1.105549182157846 \times 10^{-7}$	$7.749774527601226 \times 10^{-9}$
0.8	$4.113778074791275 \times 10^{-5}$	$4.125554726718593 \times 10^{-6}$	$3.674935878917996 \times 10^{-7}$	$2.944491394597482 \times 10^{-8}$
0.9	$9.374043008389243 \times 10^{-5}$	$1.0577612629278684 \times 10^{-5}$	$1.060155771139881 \times 10^{-6}$	$9.557343069541972 \times 10^{-8}$
1.0	$1.9582134116140592 \times 10^{-4}$	$2.45549708950409 \times 10^{-5}$	$2.734871750812168 \times 10^{-6}$	$2.739767139418478 \times 10^{-7}$

Table 8: The recurrence error of the 5th approximate solution of the imaginary part in Example 2.

τ	$\nu = 0.7$	$\nu = 0.8$	$\nu = 0.9$	$\nu = 1.0$
0.1	$1.926007539341256 \times 10^{-12}$	$1.922465206587756 \times 10^{-14}$	$1.815440978456445 \times 10^{-16}$	$1.627499919875739 \times 10^{-18}$
0.2	$3.212183277944602 \times 10^{-10}$	$6.217126403566797 \times 10^{-12}$	$1.123792369482977 \times 10^{-13}$	$1.922772907632402 \times 10^{-15}$
0.3	$6.577805665150846 \times 10^{-9}$	$1.892287752233342 \times 10^{-10}$	$5.028971037475495 \times 10^{-12}$	$1.256513068851356 \times 10^{-13}$
0.4	$5.664659911177431 \times 10^{-8}$	$2.169068535347471 \times 10^{-9}$	$7.610081091968145 \times 10^{-11}$	$2.493643660279493 \times 10^{-12}$
0.5	$3.026797519340784 \times 10^{-7}$	$1.450910885437432 \times 10^{-8}$	$6.332736016444167 \times 10^{-10}$	$2.566730381652197 \times 10^{-11}$
0.6	$1.194404986717049 \times 10^{-6}$	$6.891376017773192 \times 10^{-8}$	$3.602715131890486 \times 10^{-9}$	$1.740543007331589 \times 10^{-10}$
0.7	$3.821136878718447 \times 10^{-6}$	$2.581914817482758 \times 10^{-7}$	$1.574595275095308 \times 10^{-8}$	$8.837938438846447 \times 10^{-10}$
0.8	$1.0480156108100884 \times 10^{-5}$	$8.126788825165077 \times 10^{-7}$	$5.66988415843565 \times 10^{-8}$	$3.628126275591497 \times 10^{-9}$
0.9	$2.5548636246620873 \times 10^{-5}$	$2.238467006737139 \times 10^{-6}$	$1.759964515566688 \times 10^{-7}$	$1.265411208128710 \times 10^{-8}$
1.0	$5.674529965660330 \times 10^{-5}$	$5.548386062052328 \times 10^{-6}$	$4.85763358662764 \times 10^{-7}$	$3.879371899481992 \times 10^{-8}$

Table 9: The recurrence error of the 5th approximate solution of the real part in Example 3.

τ	$\nu = 0.7$	$\nu = 0.8$	$\nu = 0.9$	$\nu = 1.0$
0.1	$5.718354659335265 \times 10^{-11}$	$7.147943324169061 \times 10^{-13}$	$7.942159249076738 \times 10^{-15}$	$7.942159249076745 \times 10^{-17}$
0.2	$7.319493963949132 \times 10^{-9}$	$1.829873490987278 \times 10^{-10}$	$4.066385535527289 \times 10^{-12}$	$8.132771071054586 \times 10^{-14}$
0.3	$1.250604163996619 \times 10^{-7}$	$4.689765614987320 \times 10^{-9}$	$1.563255204995775 \times 10^{-10}$	$4.689765614987315 \times 10^{-12}$
0.4	$9.368952273854868 \times 10^{-7}$	$4.684476136927436 \times 10^{-8}$	$2.081989394189970 \times 10^{-9}$	$8.327957576759896 \times 10^{-11}$
0.5	$4.467464577605666 \times 10^{-6}$	$2.792165361003536 \times 10^{-7}$	$1.551202978335300 \times 10^{-8}$	$7.756014891676498 \times 10^{-10}$
0.6	$1.6007733299156725 \times 10^{-5}$	$1.200579997436754 \times 10^{-6}$	$8.003866649578365 \times 10^{-8}$	$4.802319989747010 \times 10^{-9}$
0.7	$4.709310951212926 \times 10^{-5}$	$4.120647082311310 \times 10^{-6}$	$3.204947730686570 \times 10^{-7}$	$2.243463411480599 \times 10^{-8}$
0.8	$1.1992258910534259 \times 10^{-4}$	$1.1992258910534254 \times 10^{-5}$	$1.065978569825267 \times 10^{-6}$	$8.527828558602135 \times 10^{-8}$
0.9	$2.735071306660605 \times 10^{-4}$	$3.076955219993183 \times 10^{-5}$	$3.076955219993184 \times 10^{-6}$	$2.769259697993865 \times 10^{-7}$
1.0	$5.718354659335249 \times 10^{-4}$	$7.147943324169061 \times 10^{-5}$	$7.942159249076736 \times 10^{-6}$	$7.942159249076734 \times 10^{-7}$

Table 10: The recurrence error of the 5th approximate solution of the imaginary part in Example 3.

τ	$\nu = 0.7$	$\nu = 0.8$	$\nu = 0.9$	$\nu = 1.0$
0.1	$4.044352360290241 \times 10^{-12}$	$2.95593353802917 \times 10^{-14}$	$1.896521881939167 \times 10^{-16}$	$1.083021715783192 \times 10^{-18}$
0.2	$8.40968933466814 \times 10^{-10}$	$1.317524278577765 \times 10^{-11}$	$1.811985904661213 \times 10^{-13}$	$2.218028473923979 \times 10^{-15}$
0.3	$1.908458178643264 \times 10^{-8}$	$4.670482042212528 \times 10^{-10}$	$1.003363456757901 \times 10^{-11}$	$1.918540478858446 \times 10^{-13}$
0.4	$1.748682320562088 \times 10^{-7}$	$3.375983249079892 \times 10^{-8}$	$1.731218052350544 \times 10^{-10}$	$4.542522314596309 \times 10^{-12}$
0.5	$9.748056090119807 \times 10^{-7}$	$4.184376006926562 \times 10^{-8}$	$1.576742960965881 \times 10^{-9}$	$5.288191971597613 \times 10^{-11}$
0.6	$3.968383306108540 \times 10^{-7}$	$2.081736075628826 \times 10^{-7}$	$9.586393166413172 \times 10^{-9}$	$3.929170900702099 \times 10^{-10}$
0.7	$1.3004806485065536 \times 10^{-5}$	$4.646598110881215 \times 10^{-7}$	$4.409897082301801 \times 10^{-8}$	$2.141487801867844 \times 10^{-9}$
0.8	$3.636150797676397 \times 10^{-5}$	$2.617499157554769 \times 10^{-6}$	$1.654050363788450 \times 10^{-7}$	$9.303085700293241 \times 10^{-9}$
0.9	$9.005675804590360 \times 10^{-5}$	$7.379530772932580 \times 10^{-6}$	$5.308339629215292 \times 10^{-7}$	$3.398636902083380 \times 10^{-8}$
1.0	$2.0269777712677892 \times 10^{-4}$	$1.8650679756148277 \times 10^{-5}$	$1.506460878596710 \times 10^{-6}$	$1.083021715783191 \times 10^{-7}$

Table 11: The recurrence error of the 5th approximate solution of the real part in Example 4.

τ	$\nu = 0.7$	$\nu = 0.8$	$\nu = 0.9$	$\nu = 1.0$
0.1	$1.410899077403071 \times 10^{-10}$	$1.763623846753835 \times 10^{-12}$	$1.959582051948707 \times 10^{-14}$	$1.959582051948706 \times 10^{-16}$
0.2	$1.80595081907593 \times 10^{-8}$	$4.514877047689823 \times 10^{-10}$	$1.003306010597737 \times 10^{-11}$	$2.006612021195475 \times 10^{-13}$
0.3	$3.085636282280515 \times 10^{-7}$	$1.15711360585519 \times 10^{-8}$	$3.857045352850636 \times 10^{-10}$	$1.157113605855191 \times 10^{-11}$
0.4	$2.311617048417188 \times 10^{-6}$	$1.155808524208595 \times 10^{-7}$	$5.136926774260415 \times 10^{-9}$	$2.054770709704167 \times 10^{-10}$
0.5	$1.1022649042211474 \times 10^{-5}$	$6.889155651382168 \times 10^{-7}$	$3.827308695212317 \times 10^{-8}$	$1.913654347606158 \times 10^{-9}$
0.6	$3.949614441319053 \times 10^{-5}$	$2.96221083098929 \times 10^{-6}$	$1.974807220659528 \times 10^{-7}$	$1.184884332395716 \times 10^{-8}$
0.7	$1.1619360589017545 \times 10^{-4}$	$1.0166940515390365 \times 10^{-5}$	$7.907620400859165 \times 10^{-7}$	$5.535334280601419 \times 10^{-8}$
0.8	$2.958869821974002 \times 10^{-4}$	$2.958869821974005 \times 10^{-5}$	0.000002630106508421338	$2.104085206737067 \times 10^{-7}$
0.9	$6.748286549347473 \times 10^{-4}$	$7.591822368015921 \times 10^{-5}$	$7.591822368015916 \times 10^{-6}$	$6.832640131214322 \times 10^{-7}$
1.0	$1.410899077403069 \times 10^{-3}$	$1.7636238467538362 \times 10^{-4}$	$1.959582051948707 \times 10^{-5}$	$1.959582051948706 \times 10^{-6}$

Table 12: The recurrence error of the 5th approximate solution of the imaginary part in Example 4.

τ	$\nu = 0.7$	$\nu = 0.8$	$\nu = 0.9$	$\nu = 1.0$
0.1	$1.663116214880405 \times 10^{-11}$	$1.215537262646501 \times 10^{-13}$	$7.79886620339425 \times 10^{-16}$	$4.453595572610698 \times 10^{-18}$
0.2	$3.458227535246130 \times 10^{-9}$	$5.417915641366231 \times 10^{-11}$	$7.451237851492589 \times 10^{-13}$	$9.120963732706710 \times 10^{-15}$
0.3	$7.847950572968780 \times 10^{-8}$	$1.920592896894366 \times 10^{-9}$	$4.126025345211919 \times 10^{-11}$	$7.889410949012672 \times 10^{-13}$
0.4	$7.190921222780890 \times 10^{-7}$	$2.414883590902916 \times 10^{-8}$	$7.119104761067955 \times 10^{-10}$	$1.867973372458334 \times 10^{-11}$
0.5	$4.008589930546624 \times 10^{-6}$	$1.720696657048121 \times 10^{-7}$	$6.483873192722287 \times 10^{-9}$	$2.174607213188817 \times 10^{-10}$
0.6	$1.6318762648010684 \times 10^{-5}$	$8.560502928660110 \times 10^{-7}$	$3.942110997503766 \times 10^{-8}$	$1.615751362357795 \times 10^{-9}$
0.7	$5.347828925356589 \times 10^{-5}$	$3.323770499911620 \times 10^{-6}$	$1.813435301914099 \times 10^{-7}$	$8.806213628229532 \times 10^{-9}$
0.8	$1.495255806774449 \times 10^{-4}$	$1.076366474421812 \times 10^{-5}$	$6.801776242977975 \times 10^{-7}$	$3.825609466794668 \times 10^{-8}$
0.9	$3.703308743231145 \times 10^{-4}$	$3.0346063333097793 \times 10^{-5}$	$2.182892321184059 \times 10^{-6}$	$6.832640131214322 \times 10^{-7}$
1.0	$8.335326149365687 \times 10^{-4}$	$7.669521633561604 \times 10^{-5}$	$6.194859624193012 \times 10^{-6}$	$4.453595572610698 \times 10^{-7}$

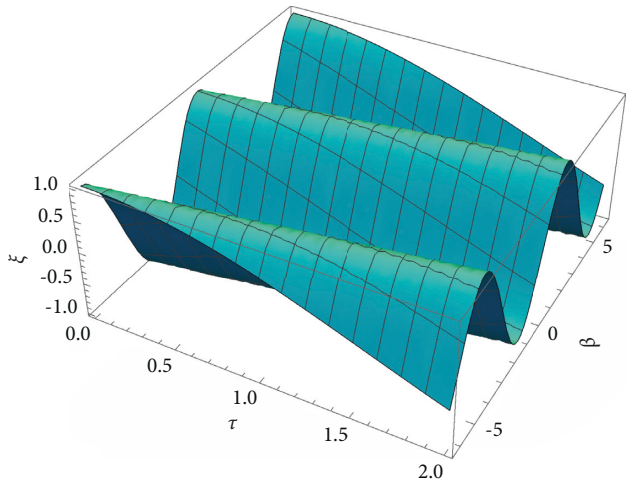

The real part of the exact solution to Example 1.

Figure 17: The real part of the exact solution to Example 1.

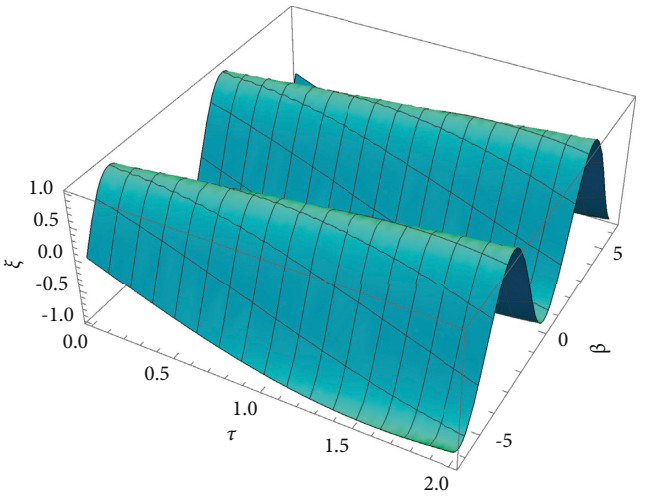

The imaginary part of the exact solution to Example 1.

Figure 18: The imaginary part of the exact solution to Example 1.

efficient algorithm for solving fractional-order differential equations with fewer calculations and iteration steps.

The following are the 3D graphs for the real and imaginary parts of the exact solution to Example 2:

The real and imaginary parts of the exact solution equation (51) at $\nu = 1$ are shown in Figures 19 and 20 respectively in the intervals $\tau \in [0, 2]$, and $\varpi \in [-2\pi, 2\pi]$.

The following 2D graphs show the real and imaginary parts of approximate and exact solutions to Example 3:

Figures 5 and 6 show the behavior of the real and imaginary parts in the interval $\tau \in [0, 1]$ between the 5th step iteration approximate and exact solutions of equation (60) at several values of ν when $\varpi = 0.05$. The approximate result corresponds with the precise result at $\nu = 1$ and this proves the effectiveness and precision of the suggested method.

The 2D graphs of absolute error for the real and imaginary parts of the 5th approximation and exact solutions to Example 3 are as follows:

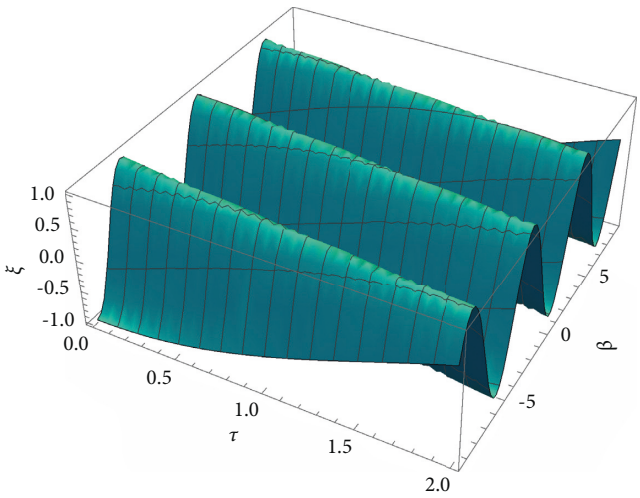

The real part of the exact solution to Example 2.

Figure 19: The real part of the exact solution to Example 2.

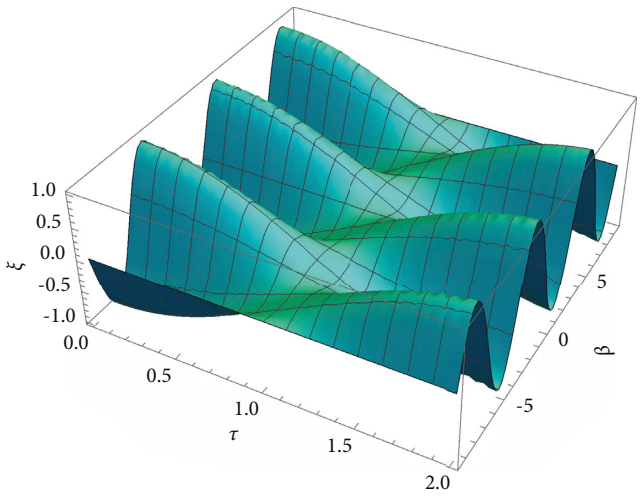

The real part of the exact solution to Example 3.

Figure 21: The real part of the exact solution to Example 3.

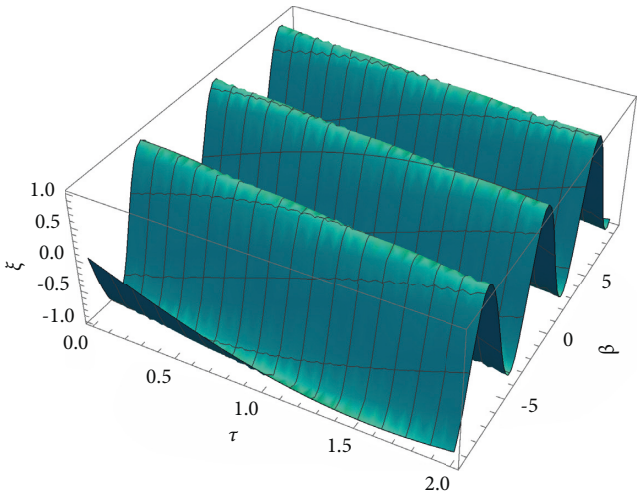

The imaginary part of the exact solution to Example 2.

Figure 20: The imaginary part of the exact solution to Example 2.

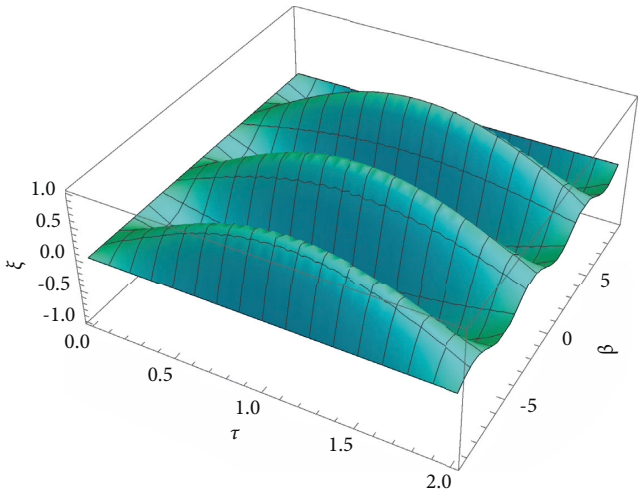

The imaginary part of the exact solution to Example 3.

Figure 22: The imaginary part of the exact solution to Example 3.

Figures 11 and 12 demonstrate the 2D graph of real and imaginary parts of absolute error in the intervals $\tau \in [0, 1]$ when $\varpi = 0.05$ are over the 5th terms approximate and exact solutions of equation (60) at $\nu = 1$. As for the figures, approximate and precise solutions are in very good agreement.

Table 3 shows comparisons of the real and imaginary parts of the absolute error of the 5th approximate solution obtained by ATDM of Example 3 at $\nu = 1$ with the absolute error of approximate solutions obtained by HPM [35]. The results obtained from the suggested method are extremely similar to those obtained by HPM.

The recurrence error $|\xi^5(\varpi, \tau) - \xi^4(\varpi, \tau)|$ between the 5th and 4th approximate solution of the real part with different values of ν, when $\varpi = 0.05$ for Example 3 are presented as follows:

The recurrence error $|\xi^5(\varpi, \tau) - \xi^4(\varpi, \tau)|$ between the 5th and 4th approximate solution of the imaginary part with different values of ν, when $\varpi = 0.05$ for Example 3 are presented as follows:

The convergence of the ATDM of real and imaginary of the approximate solution to the exact solution for equation (60) has been shown numerically as in Tables 9 and 10. The results show that the proposed technique is a useful and efficient algorithm for solving fractional-order differential equations with fewer calculations and iteration steps.

The following are 3D graphs for the real and imaginary parts of the exact solution to Example 3:

The real and imaginary parts of the exact solution equation (60) at $\nu = 1$ are shown in Figures 21 and 22, respectively, in the intervals $\tau \in [0, 2], \varpi \in [-3\pi, 3\pi]$.

The following 2D graphs show the real and imaginary parts of approximate and exact solutions to Example 4:

Figures 7 and 8 show the behavior of the real and imaginary parts in the interval $\tau \in [0, 1]$ between the 5th step iteration approximate and exact solutions of equation

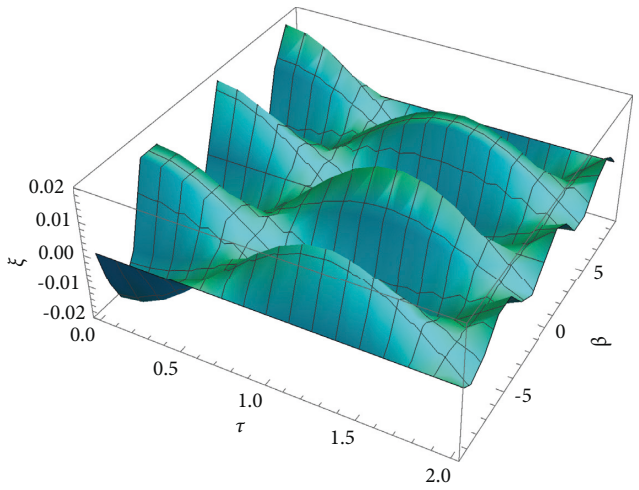

Figure 23: The real part of the exact solution to Example 4.

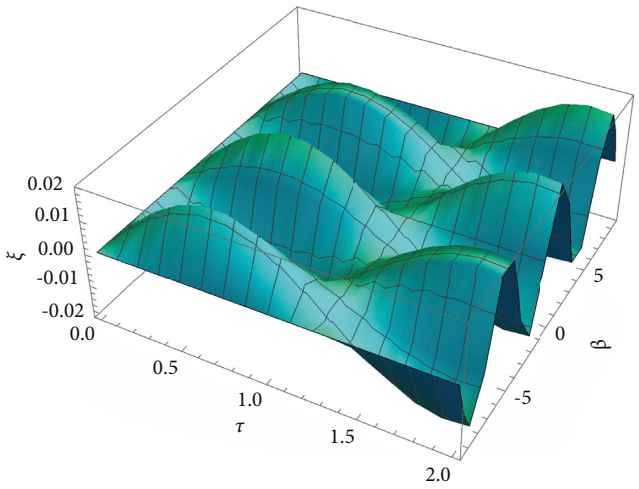

Figure 24: The imaginary part of the exact solution to Example 4.

(71) at several values of ν when $\varpi = 0.05$, $\beta = 0.10$, and $\mu = 0.15$. The approximate result corresponds with the precise result at $\nu = 1$ and this proves the effectiveness and precision of the recommended method.

The 2D graphs of absolute error for the real and imaginary parts of the 5th approximation and exact solutions to Example 4 are as follows:

Figures 15 and 16 demonstrate the 2D graph of real and imaginary parts of absolute error in the intervals $\tau \in [0, 1]$ when $\varpi = 0.05$, $\beta = 0.10$, and $\mu = 0.15$ are over the 5th terms approximate and exact solutions of equation (71) at $\nu = 1$. As for the figures, approximate and precise solutions are in very good agreement.

Table 4 shows comparisons of the real and imaginary parts of the absolute error of the 5th approximate solution obtained by ATDM of Example 4 at $\nu = 1$ with the absolute error of the approximate solution obtained by HAM [43]. The results obtained from the suggested method are extremely similar to those obtained by HAM.

The recurrence error $|\xi^5(\varpi, \beta, \mu, \tau) - \xi^4(\varpi, \beta, \mu, \tau)|$ between the 5th and 4th approximate solution of the real part with different values of ν, when $\varpi = 0.05$, $\beta = 0.10$, and $\mu = 0.15$ for Example 4 are presented.

The recurrence error $|\xi^5(\varpi, \beta, \mu, \tau) - \xi^4(\varpi, \beta, \mu, \tau)|$ between the 5th and 4th approximate solutions of the imaginary part with different values of ν, when $\varpi = 0.05$, $\beta = 0.10$, and $\mu = 0.15$ for Example 4 are presented.

The convergence of the ATDM of real and imaginary of the approximate solution to the exact solution for equation (71) has been shown numerically as in Tables 11 and 12. The results show that the proposed technique is a useful and efficient algorithm for solving fractional-order differential equations with fewer calculations and iteration steps.

The following are 3D graphs for the real and imaginary parts of the exact solution to Example 4:

The real and imaginary parts of the exact solution equation (71) at $\nu = 1$ are shown in Figures 23 and 24 respectively in the intervals $\tau \in [0, 2], \varpi \in [-3\pi, 3\pi]$ with $\beta = 0.1$ and $\mu = 0.2$.

6. Conclusion

The Aboodh transform decomposition method is effectively used in this study to obtain analytical approximate and exact solutions to time-fractional linear and nonlinear Schrodinger equations with zero and nonzero trapping potential that are regarded in the Caputo sense. The Aboodh transform is more closely related to the Laplace and Elzaki transforms. The Aboodh transform is a useful method for solving time-domain differential equations. The recurrence and absolute error of the four problems are analyzed to evaluate the efficiency and consistency of the presented method. In addition, numerical results are also compared with other methods such as the fractional reduced differential transform method (FRDTM), the homotopy analysis method (HAM), and the homotopy perturbation method (HPM). The results obtained by the proposed method show excellent agreement with these methods, which indicates its effectiveness and reliability. This method has the advantage of needing no assumptions regarding minor or important physical parameters in the problem. As a result, it can solve both weakly and strongly nonlinear problems, overcoming some of the drawbacks of traditional perturbation methods. Only a few computations are required to solve nonlinear fractional-order differential equations. As a result, it greatly improves homotopy analysis and homotopy perturbation techniques. The ATDM can construct expansion solutions for linear and nonlinear fractional-order differential equations without the requirement for perturbation, linearization, or discretization, unlike earlier analytic approximation methods.

Therefore, we concluded that our proposed technique is simple to apply, accurate, and efficient according to the results. It is significant to consider that implementing the ATDM to solve other kinds of ordinary and partial DEs of noninteger order is actively attainable. For example,

fractional kdv equations, fractional phi-4 equations, fractional Schrodinger equations, and many more.

Data Availability

No data were generated or analyzed during the current study.

Conflicts of Interest

The authors declare that they have no competing interests.

Authors' Contributions

The authors declare that the study was realized in collaboration with equal responsibility. All authors read and approved the final manuscript.

References

[1] A. K. Mittal and L. K. Balyan, "Numerical solutions of two-dimensional fractional Schrodinger equation," *Mathematical Sciences*, vol. 14, no. 2, pp. 129–136, 2020.

[2] A. Liemert and A. Kienle, "Fractional Schrödinger equation in the presence of the linear potential," *Mathematics*, vol. 4, no. 2, p. 31, 2016.

[3] X. Guo and M. Xu, "Some physical applications of fractional Schrödinger equation," *Journal of Mathematical Physics*, vol. 47, no. 8, Article ID 082104, 2006.

[4] J. Wang, Y. Zhou, and W. Wei, "Fractional Schrödinger equations with potential and optimal controls," *Nonlinear Analysis: Real World Applications*, vol. 13, no. 6, pp. 2755–2766, 2012.

[5] S. Kumar, M. Niwas, and A. M. Wazwaz, "Lie symmetry analysis, exact analytical solutions and dynamics of solitons for (2+1)-dimensional NNV equations," *Physica Scripta*, vol. 95, no. 9, Article ID 095204, 2020.

[6] W. X. Ma, "Inverse scattering for nonlocal reverse-time nonlinear Schrödinger equations," *Applied Mathematics Letters*, vol. 102, Article ID 106161, 2020.

[7] M. A. Zaky, "An accurate spectral collocation method for nonlinear systems of fractional differential equations and related integral equations with nonsmooth solutions," *Applied Numerical Mathematics*, vol. 154, pp. 205–222, 2020.

[8] N. K. Vitanov and Z. I. Dimitrova, "Simple equations method (SEsM) and its particular cases: Hirota method," *AIP Conference Proceedings*, vol. 2321, no. 1, Article ID 030036, 2021.

[9] R. Hassan, M. El-Agamy, M. S. A. Latif, and H. Nour, "On Backlund transformation of Riccati equation method and its application to nonlinear partial differential equations and differential-difference equations," *Open Journal of Mathematical Sciences*, vol. 4, no. 1, pp. 56–62, 2020.

[10] D. Kumar, A. R. Seadawy, and A. K. Joardar, "Modified Kudryashov method via new exact solutions for some conformable fractional differential equations arising in mathematical biology," *Chinese Journal of Physics*, vol. 56, no. 1, pp. 75–85, 2018.

[11] D. Rani and V. Mishra, "Modification of Laplace Adomian decomposition method for solving nonlinear Volterra integral and integro-differential equations based on Newton Raphson formula," *European Journal of Pure and Applied Mathematics*, vol. 11, no. 1, pp. 202–214, 2018.

[12] A. Khan, M. I. Liaqat, M. Younis, and A. Alam, "Approximate and exact solutions to fractional order Cauchy reaction-diffusion equations by new combine techniques," *Journal of Mathematics*, vol. 2021, Article ID 5337255, 12 pages, 2021.

[13] M. I. Liaqat, A. Khan, and A. Akgül, "Adaptation on power series method with conformable operator for solving fractional order systems of nonlinear partial differential equations," *Chaos, Solitons & Fractals*, vol. 157, Article ID 111984, 2022.

[14] M. Ur Rehman and R. Ali Khan, "The Legendre wavelet method for solving fractional differential equations," *Communications in Nonlinear Science and Numerical Simulation*, vol. 16, no. 11, pp. 4163–4173, 2011.

[15] M. I. Liaqat, A. Khan, M. A. Alam, M. K. Pandit, S. Etemad, and S. Rezapour, "Approximate and closed-form solutions of Newell-Whitehead-Segel equations via modified conformable Shehu transform decomposition method," *Mathematical Problems in Engineering*, vol. 2022, Article ID 6752455, 14 pages, 2022.

[16] H. M. Ozaktas and M. A. Kutay, "The fractional Fourier transforms," in *Proceedings of the 2001 European Control Conference (ECC)*, pp. 1477–1483, IEEE, Porto, Portugal, September 2001.

[17] Y. Z. Povstenko, "Fractional heat conduction equation and associated thermal stress," *Journal of Thermal Stresses*, vol. 28, no. 1, pp. 83–102, 2004.

[18] L. Kexue and P. Jigen, "Laplace transform and fractional differential equations," *Applied Mathematics Letters*, vol. 24, no. 12, pp. 2019–2023, 2011.

[19] S. Kazem, "Exact solution of some linear fractional differential equations by Laplace transform," *International Journal of Nonlinear Science*, vol. 16, no. 1, pp. 3–11, 2013.

[20] S. Kumar, "A new analytical modelling for fractional telegraph equation via Laplace transform," *Applied Mathematical Modelling*, vol. 38, no. 13, pp. 3154–3163, 2014.

[21] Z. B. Li and J. H. He, "Fractional complex transform for fractional differential equations," *Mathematical and Computational Applications*, vol. 15, no. 5, pp. 970–973, 2010.

[22] H. Zhang, "A note on some sub-equation methods and new types of exact travelling wave solutions for two nonlinear partial differential equations," *Acta Applicandae Mathematica*, vol. 106, no. 2, pp. 241–249, 2009.

[23] T. M. Elzaki, "Application of new transform "Elzaki transform" to partial differential equations," *Global Journal of Pure and Applied Mathematics*, vol. 7, no. 1, pp. 65–70, 2011.

[24] A. Kiliçman, H. Eltayeb, and R. P. Agarwal, "On Sumudu transform and system of differential equations," *Abstract and Applied Analysis*, vol. 2010, Article ID 598702, 2010.

[25] L. Riabi, K. Belghaba, M. H. Cherif, and D. Ziane, "Homotopy perturbation method combined with ZZ transform to solve some nonlinear fractional differential equations," *International Journal of Analysis and Applications*, vol. 17, no. 3, pp. 406–419, 2019.

[26] K. S. Aboodh, "The new integral transform Aboodh transform," *Global Journal of Pure and Applied Mathematics*, vol. 9, no. 1, pp. 35–43, 2013.

[27] R. M. Jena and S. Chakraverty, "Q-homotopy analysis Aboodh transform method based solution of proportional delay time-fractional partial differential equations," *Journal of Interdisciplinary Mathematics*, vol. 22, no. 6, pp. 931–950, 2019.

[28] S. Rashid, K. T. Kubra, and J. L. G. Guirao, "Construction of an approximate analytical solution for multi-dimensional fractional Zakharov–Kuznetsov equation via Aboodh

Adomian decomposition method," *Symmetry*, vol. 13, no. 8, p. 1542, 2021.

[29] G. T. Tukaram and R. G. Anantha, "On Aboodh transform for fractional differential operator," *Malaya Journal of Matematik*, vol. 8, no. 1, pp. 225–229, 2020.

[30] G. O. Ojo and N. I. Mahmudov, "Aboodh transform iterative method for spatial diffusion of a biological population with fractional-order," *Mathematics*, vol. 9, no. 2, p. 155, 2021.

[31] M. A. Awuya and D. Subasi, "Aboodh transform iterative method for solving fractional partial differential equation with Mittag–Leffler Kernel," *Symmetry*, vol. 13, no. 11, p. 2055, 2021.

[32] Q. T. Ain, J. H. He, N. Anjum, and M. Ali, "The fractional complex transform: a novel approach to the time-fractional Schrödinger equation," *Fractals*, vol. 28, no. 7, Article ID 2050141, 2020.

[33] A. H. Bhrawy, J. F. Alzaidy, M. A. Abdelkawy, and A. Biswas, "Jacobi spectral collocation approximation for multi-dimensional time-fractional Schrödinger equations," *Nonlinear Dynamics*, vol. 84, no. 3, pp. 1553–1567, 2016.

[34] B. Hicdurmaz and A. Ashyralyev, "A stable numerical method for multidimensional time fractional Schrödinger equations," *Computers & Mathematics with Applications*, vol. 72, no. 6, pp. 1703–1713, 2016.

[35] A. Khalili Golmankhaneh, "Solving of the fractional nonlinear and linear Schrodinger equations by homotopy perturbation method," 2008, https://arxiv.org/abs/0809.

[36] B. Ghanbari, "Abundant exact solutions to a generalized nonlinear Schrödinger equation with local fractional derivative," *Mathematical Methods in the Applied Sciences*, vol. 44, no. 11, pp. 8759–8774, 2021.

[37] Y. Zhang, A. Kumar, S. Kumar, D. Baleanu, and X. J. Yang, "Residual power series method for time-fractional Schrödinger equations," *Journal of Nonlinear Sciences and Applications*, vol. 9, no. 11, pp. 5821–5829, 2016.

[38] S. O. Edeki, G. O. Akinlabi, and S. A. Adeosun, "On a modified transformation method for exact and approximate solutions of linear Schrödinger equations," *AIP Conference proceedings*, vol. 1705, no. 1, Article ID 020048, 2016.

[39] A. Ravi Kanth and K. Aruna, "Two-dimensional differential transform method for solving linear and non-linear Schrödinger equations," *Chaos, Solitons & Fractals*, vol. 41, no. 5, pp. 2277–2281, 2009.

[40] D. Lu, A. Seadawy, and M. Arshad, "Applications of extended simple equation method on unstable nonlinear Schrödinger equations," *Optik*, vol. 140, pp. 136–144, 2017.

[41] A. R. Hadhoud, A. A. M. Rageh, and T. Radwan, "Computational solution of the time-fractional Schrödinger equation by using trigonometric B-spline collocation method," *Fractal and Fractional*, vol. 6, no. 3, p. 127, 2022.

[42] B. K. Singh and P. Kumar, "A new approximate solution of time-fractional, non-linear Schrodinger equations using fractional reduced differential transformation," 2016, https://arxiv.org/abs/1611.07171.

[43] A. K. Alomari, M. S. M. Noorani, and R. Nazar, "Explicit series solutions of some linear and nonlinear Schrodinger equations via the homotopy analysis method," *Communications in Nonlinear Science and Numerical Simulation*, vol. 14, no. 4, pp. 1196–1207, 2009.

[44] V. V. Kulish and J. L. Lage, "Application of fractional calculus to fluid mechanics," *Journal of Fluids Engineering*, vol. 124, pp. 803–806, 2002.

[45] Y. A. Rossikhin and M. V. Shitikova, "Application of fractional calculus for dynamic problems of solid mechanics: novel trends and recent results," *Applied Mechanics Reviews*, vol. 63, no. 1, 2010.

[46] K. Manimegalai, C. F. S. Zephania, P. K. Bera, P. Bera, S. K. Das, and T. Sil, "Study of strongly nonlinear oscillators using the Aboodh transform and the homotopy perturbation method," *The European Physical Journal Plus*, vol. 134, no. 9, pp. 462–510, 2019.

[47] H. M. Fahad and A. Fernandez, "Operational calculus for Caputo fractional calculus with respect to functions and the associated fractional differential equations," *Applied Mathematics and Computation*, vol. 409, Article ID 126400, 2021.